Journal of Medicinal Chemistry

ARTICLE

pubs.acs.org/jmc

# Pyrazolo[4,3-*d*]pyrimidine Bioisostere of Roscovitine: Evaluation of a Novel Selective Inhibitor of Cyclin-Dependent Kinases with Antiproliferative Activity†

Radek Jorda,[‡] Libor Havlíček,[‡,§] Iain W. McNae,[∥] Malcolm D. Walkinshaw,[∥] Jiří Voller,[⊥] Antonín Šturc,[‡] Jana Navrátilová,[‡] Marek Kuzma,[#] Martin Mistrík,[∞] Jiří Bártek,[∞] Miroslav Strnad,[‡] and Vladimír Kryštof*[,‡]

[‡]Laboratory of Growth Regulators, Faculty of Science, Palacký University and Institute of Experimental Botany ASCR, Šlechtitelů 11, 78371 Olomouc, Czech Republic

[§]Isotope Laboratory, Institute of Experimental Botany ASCR, Videnska 1083, 142 20 Prague, Czech Republic

[∥]Structural Biochemistry Group, University of Edinburgh, Michael Swann Building, King's Buildings, Edinburgh, EH9 3JR, Scotland

[⊥]Centre of the Region Haná for Biotechnological and Agricultural Research, Faculty of Science, Department of Growth Regulators, Palacký University, Šlechtitelů 11, Olomouc, CZ-783 71, Czech Republic

[#]Laboratory of Molecular Structure Characterization, Institute of Microbiology ASCR, Videnska 1083, 142 20 Prague, Czech Republic

[∞]Laboratory of Genome Integrity and Institute of Molecular and Translational Medicine, Palacký University, Šlechtitelů 11, 78371 Olomouc, Czech Republic

Supporting Information

**ABSTRACT:** Inhibition of cyclin-dependent kinases (CDKs) with small molecules has been suggested as a strategy for treatment of cancer, based on deregulation of CDKs commonly found in many types of human tumors. Here, a new potent CDK2 inhibitor with pyrazolo[4,3-*d*]pyrimidine scaffold has been synthesized, characterized, and evaluated in cellular and biochemical assays. 7-Benzylamino-5(*R*)-[2-(hydroxymethyl)-propyl]amino-3-isopropyl-1(2)*H*-pyrazolo[4,3-*d*]pyrimidine, compound **7**, was prepared as a bioisostere of the well-known CDK inhibitor roscovitine. An X-ray crystal structure of compound **7** bound to CDK2 has been determined, revealing a binding mode similar to that of roscovitine. Protein kinase selectivity profile of compound **7** and its biological effects (cell cycle arrest, dephosphorylation of the retinoblastoma protein, accumulation of the tumor suppressor protein p53, induction of apoptosis, inhibition of homologous recombination) are consistent with CDK inhibition as a primary mode of action. Importantly, as the anticancer activities of the pyrazolo[4,3-*d*]pyrimidine **7** exceed those of its bioisostere roscovitine, compound **7** reported here may be preferable for cancer therapy.

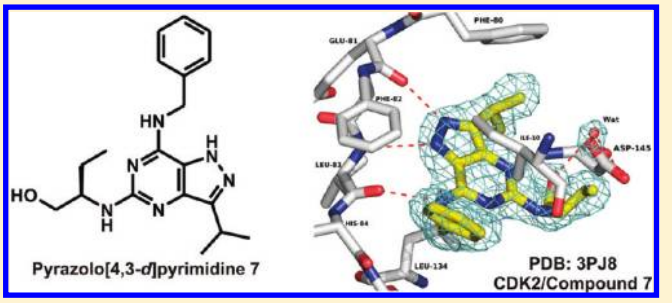


## INTRODUCTION

A growing body of evidence has linked abnormal protein phosphorylation patterns with pathogenesis of various human diseases and encouraged the search for compounds capable of specifically inhibiting protein kinases. Indeed, therapeutic success of several kinase inhibitors that had been approved for the treatment of particular cancer type(s) during recent years established protein kinases as an important class of novel drug targets. Among the 518 human genes encoding protein kinases, cyclin-dependent protein kinases (CDKs) have originally attracted attention because of their frequent deregulation in cancer.[1,2] Cyclin-dependent kinases, listing at least 13 members in humans, are serine/threonine kinases that participate mainly in processes of cell cycle control, transcription, and postranscriptional modifications but also in cell differentiation and cell death.[3,4]

During the past decade many CDK inhibitors have been developed and characterized. Some of the most efficient ones entered clinical trials as candidate drugs against various types of cancer[5,6] and/or advanced to preclinical evaluation of potential value in treatment of other diseases linked with CDK deregulation, such as neurodegenerative and cardiac disorders, viral and protozoan infections, glomerulonephritis or other types of chronic inflammation.[3,7−10] The purine heterocycle became one of the first systematically investigated scaffolds of CDK inhibitors (due to a possibility of variable substitutions mainly at positions 2, 6, and 9), leading to the discoveries of olomoucine and roscovitine.[11−13] Roscovitine is a pan-selective CDK

**Received:** January 21, 2011
**Published:** March 21, 2011

  

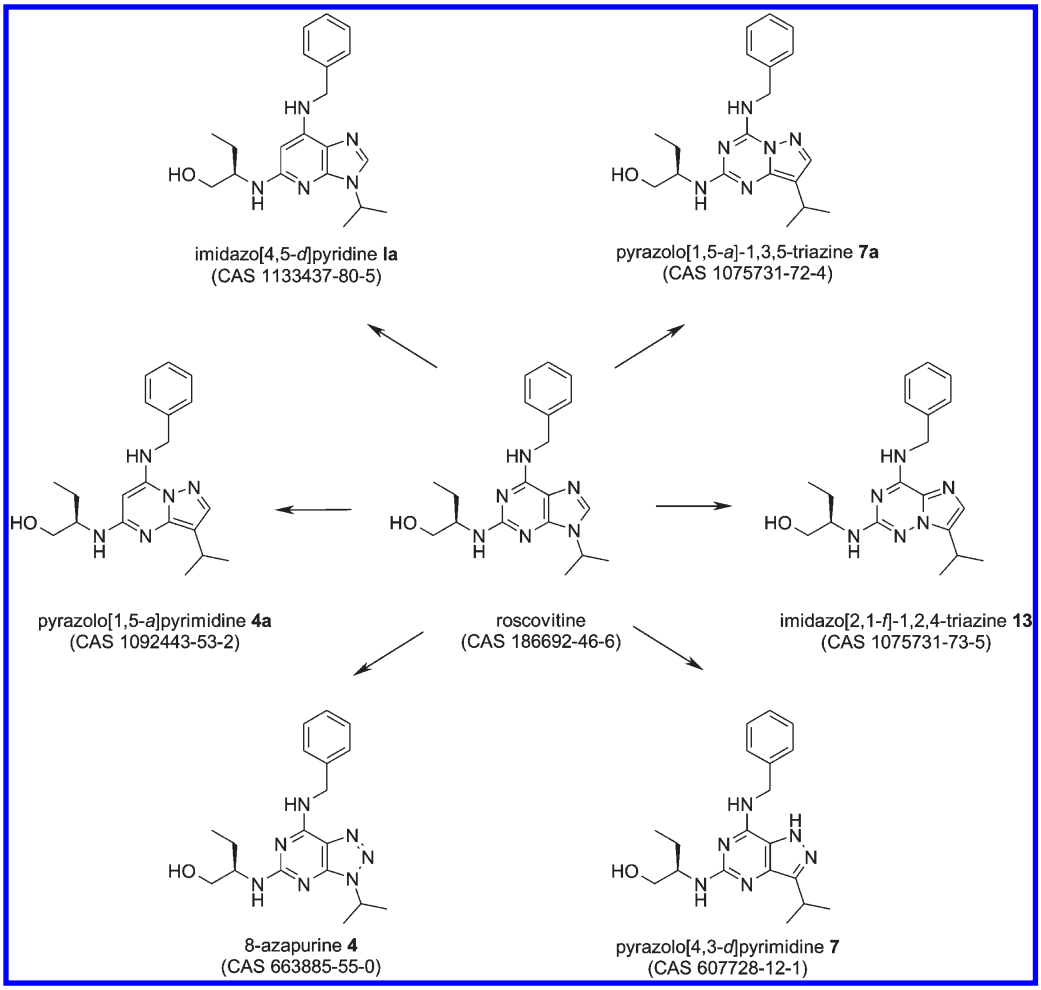


**Figure 1.** Structure of roscovitine and its known bioisosteres.[26,30,39,42] CAS numbers indicate Chemical Abstracts Service compound identifiers.

inhibitor with multiple effects on cell proliferation, cell cycle progression, p53 expression, and p53-dependent transcription and/or induction of apoptosis in cancer cells.[14] Because of these effects, (*R*)-roscovitine was among the first CDK inhibitors that entered clinical trials.

Inspired by the success of roscovitine, further exploration of purine-derived CDK inhibitors has been mainly oriented toward either modifications of the roscovitine molecule in its substitutable positions or, more recently, redistribution of nitrogen atoms of the purine scaffold. Both these directions have led not only to the large number of purine inhibitors derived from roscovitine[15−22] but also to libraries of compounds with alternative core heterocyclic skeleton structure with side chain types of roscovitine: pyrazolo[3,4-*d*]pyrimidines,[23,24] pyrazolo[1,5-*a*]-1,3,5-triazines,[25−27] imidazo[2,1-*f*]-1,2,4-triazines,[25,26] pyrazolo-[1,5-*a*]pyrimidines,[28−34] imidazo[1,2-*a*]pyrazines,[35,36] triazolo-[1,5-*a*]pyrimidines,[37,38] imidazo[4,5-*d*]pyridines[39] and pyrolo-[3,2-*d*]pyrimidines.[40]

In this study, we describe synthesis of a novel bioisostere of roscovitine with the pyrazolo[4,3-*d*]pyrimidine core. The 3,7-disubstituted pyrazolo[4,3-*d*]pyrimidines were previously described as CDK inhibitors,[41] and we have found that introduction of the third substituent to position 5 led to development of a new class of potent purine-related CDK inhibitors. The representative 3,5,7-trisubstituted pyrazolo[4,3-*d*]pyrimidine **7** has been evaluated in diverse biological assays in comparison with roscovitine as a reference molecule. Our results demonstrate that a change in a position of a single nitrogen atom can alter CDK inhibitory properties of this class of compounds, analogous to some other purine bioisosteres (Figure 1).[23,25,26,33,39,42]

## RESULTS AND DISCUSSION

**Chemistry.** We have previously described synthesis of 5,7-di(4-methoxybenzyl)amino-3-isopropyl-1(2)*H*-pyrazolo[4,3-*d*]pyrimidine that was prepared as an analogue of microtubule-interfering drug myoseverin.[43] A key assumed intermediate of the synthetic route was 5,7-dichloro-3-isopropyl-1(2)*H*-pyrazolo[4,3-*d*]pyrimidine. However the intermediate was not isolated and characterized. An attempt to synthesize pyrazolo-[4,3-*d*]pyrimidine analogue of roscovitine, i.e., the compound with different 5,7-substituents in contrast to 5,7-disubstituted myoseverin derivative, via the same synthetic approach was not successful. Therefore, we developed a completely new synthetic route outlined in Scheme 1. This synthetic approach is simple, and all intermediates are easily detectable and isolatable, with the exception of the final compound **7**. The last reaction step gives only poor yield of the desired compound even in a complex reaction mixture, and therefore, compound **7** has to be isolated by a column chromatography.

**Scheme 1**

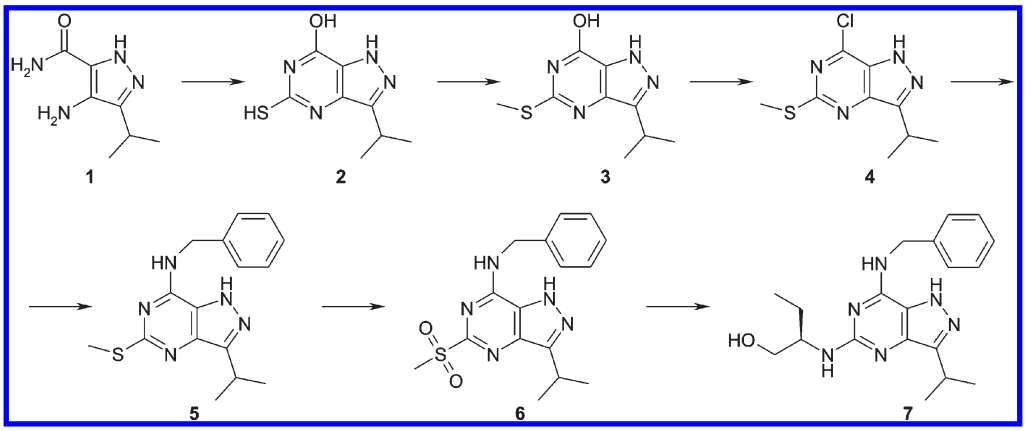

**Table 1. Inhibition of Proliferation in a Panel of Human Cancer Cell Lines by Compound 7**

| human tumor cell lines | | |
|---|---|---|
| origin | type | $IC_{50}$ ($\mu$M),[a] 7 |
| breast | MCF-7 | 7.5 ± 2.3 |
| | HBL-100 | 11.3 ± 2.4 |
| | BT-474 | 8.5 ± 0.5 |
| colon | HT-29 | 6.6 ± 1.9 |
| | HCT-116 | 11.0 ± 1.8 |
| multiple myeloma | RPMI-8226 | 3.6 ± 0.3 |
| | U266 | 4.9 ± 0.1 |
| leukemia | K-562 | 7.7 ± 0.8 |
| | CEM | 3.8 ± 0.8 |
| | HL-60 | 7.1 ± 0.5 |
| osteosarcoma | HOS | 7.5 ± 1.9 |
| melanoma | G-361 | 4.8 ± 1.6 |
| cervix | HeLa | 6.9 ± 1.7 |
| lung | A-549 | 7.1 ± 2.1 |
| epidermis | A-431 | 7.7 ± 0.3 |

[a] Average ± SD values from three determinations.

**Anticancer Cytotoxicity.** For a comparison of pyrazolo[4,3-*d*]-pyrimidines with purines, the antiproliferative activity of compound 7 was tested on a panel of human cell lines representing a range of tumor types (Table 1). Determination of proliferation clearly showed stronger activity of compound 7 over roscovitine. This result was further confirmed through testing on the NCI60 panel (Figure S2 in Supporting Information),[44] where compound 7 showed a higher activity than both racemic *R,S*-roscovitine and *R*-roscovitine in all three assay end points ($GI_{50}$, TGI, $LC_{50}$) (Table 2). All the observed differences in the activity are statistically highly significant ($p < 10^{-7}$, one-sided Wilcoxon paired test). In contrast to roscovitine, compound 7 showed not only cytostatic ($GI_{50}$, TGI) but also significant cytotoxic ($LC_{50}$) effect against the majority (74.6%) of the NCI60 cell lines in the concentration range applied. The observed comparable median activities of compound 7 toward the cell lines with either the wild-type or mutant p53 (7.5 vs 10.4, 23.2 vs 26.4, and 55.8 vs 66.5 $\mu$M for $GI_{50}$, TGI, and $LC_{50}$, respectively) are consistent with the accepted opinion that p53 status does not play a major role in resistance to CDK inhibitors.[45−47]

In order to identify compounds with similar effects on the NCI60 cell lines, we calculated Pearson correlation coefficients ($r$) of the activity patterns ($GI_{50}$ values for the individual cell lines) of compound 7 and 16 533 other compounds tested on the NCI60 panel (see Experimental Section for the criteria of compound selection). Calculations were carried out on a log−log scale. The analysis identified 2*H*-pyrazolo[3,4-*d*]-pyrimidine CGP-57380[48] ($r$ = 0.66, rank 1, $p = 1.0 \times 10^{-8}$), an inhibitor of MNK1. MNK1 is a positive regulator of the eukaryotic initiation factor 4E (eIF4E), which besides its role in translation also regulates distribution of cyclin D1 mRNA.[49] Treatment with MNK1 inhibitor leads to a decrease of the cellular content of cyclin D1.[49,50] A strong correlation was observed for the cells with both the wild type ($N$ = 16, $r$ = 0.71, $p$ = 0.0022) and mutant p53 gene ($N$ = 43, $r$ = 0.63, $p = 7.0 \times 10^{-6}$). It is tempting to speculate that the observed similarity in the activity patterns of the two compounds might stem from an effect on CDK activity, directly in the case of compound 7 and indirectly in the case of MNK1 inhibitor. On the other hand, comparison with experimentally validated ($IC_{50}$ < 100 $\mu$M) inhibitors of cyclin-dependent kinases 1 and 2 and related kinases (CDKs 4, 5, 7, 8, 9 and/or glycogen synthase kinase-3$\beta$) included in BindingDB (33 compounds, 37 activity patterns)[51,52] shows that $GI_{50}$ pattern of compound 7 is distinctly different. This observation suggests that other factors beyond the known shared molecular target(s) influence the resulting biological activity. Figure 2 shows signed coefficients of determination $r^2$ (measure of variability explained by a regression line) calculated separately for the cell lines with the wild-type and mutant p53 gene. The cumulation of the data points along the $x$ axis indicates various degrees of similarity in the activity of compound 7 and the individual CDK/GSK3B inhibitors against the cell lines expressing wild-type p53. On the other hand, the activity pattern of compound 7 on the p53 mutant cell lines was distinctly different (low signed $r^2$). A possible explanation of this difference might be a generally high sensitivity of certain p53 wild type cell lines to chemical insults. Similar results were obtained when rank sum correlation was used instead of Pearson's correlation for calculation of signed coefficient of determination (not shown). We conclude that growth inhibitory activity of compound 7 differs

Table 2. Cytostatic and Cytotoxic Effects of Compound 7 and *R,S*- and *R*-Roscovitine against NCI60 Panel[a]

| | $GI_{50}$ ($\mu$M) | | TGI ($\mu$M) | | $LC_{50}$ ($\mu$M) | |
|---|---|---|---|---|---|---|
| | median | range | median | range | median | range |
| 7 | 10.2 | 3.0−23.8 (0/59) | 25.9 | 10.6−60.8 (0/59) | 65.3 | 39.1 to >100 (15/59) |
| *R,S*-roscovitine | 17.9 | 4.6−57.8 (0/59) | 58.1 | 20.9 to >100 (14/59) | >100 | 51.9 to >100 (39/59) |
| *R*-roscovitine | 19.3 | 4.9 to >100 (1/52) | >100 | 14 to >100 (36/53) | >100 | 82.0 to >100 (50/53) |

[a] Given are median and range of $GI_{50}$, TGI, and $LC_{50}$ together with proportion of the cell lines for which the end point was not reached at the highest concentration tested (100 $\mu$M) (data in parentheses).

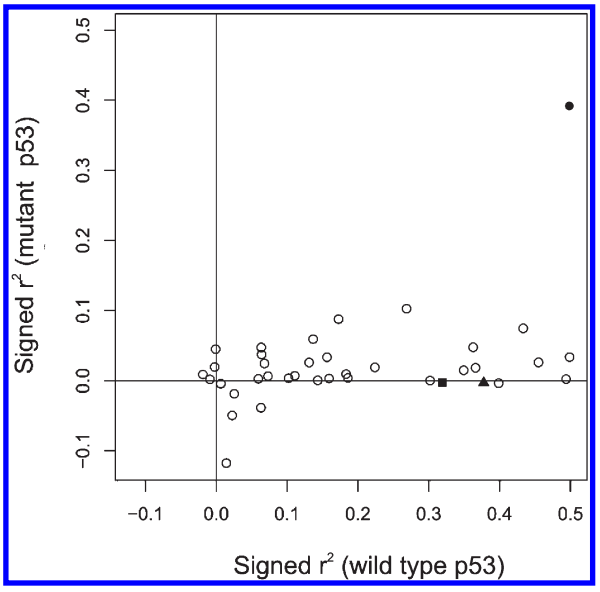


**Figure 2.** Effect of p53 status on relation (expressed as signed coefficient of determination $r^2$) between $GI_{50}$ patterns of compound 7 and individual inhibitors of CDKs and/or GSK3B. Black circle designates MNK-1 inhibitor.[48] Black triangle designates *R*-roscovitine, and black square designates racemic roscovitine.

from those of other structurally diverse CDK inhibitors, including its isomer roscovitine, and this difference is typically more pronounced when only the cell lines harboring mutant p53 are considered.

**Kinase Selectivity of Compound 7.** The kinase selectivity of compound 7 was determined in enzyme assays with recombinant CDK2/cyclin E, CDK5/p35, CDK7/cyclin H/MAT1, and CDK9/cyclin T1. The $IC_{50}$ values for compound 7 were comparable to that of roscovitine (Table 3), but isomer 7 showed generally better efficiency in CDK inhibition with $IC_{50}$ values in the submicromolar range (Figure S1). In the following experiment the selectivity of compound 7 was tested against a panel of purified recombinant human protein kinases at a single concentration of 10 $\mu$M. The assays confirmed that compound 7 inhibits preferentially CDKs (Table 3). In addition to potent inhibition of CDKs, moderate inhibition was observed for GSK3B, stress-activated protein kinases PRAK and MSK1, and mitogen-activated kinase MEK, and these activities may contribute to the observed antiproliferative effects of compound 7.

**Crystal Structure of Compound 7 with CDK2.** The crystal structure of compound 7 in complex with CDK2 has been determined at 1.96 Å resolution. Compound 7 binds in the narrow cleft between the N- and C-terminal domains of CDK2.

Table 3. Kinase Selectivity Profile for Compound 7 and Its Purine Analogue Roscovitine

| | kinase inhibition (%)[a] | | $IC_{50}$ ($\mu$M)[b] | |
|---|---|---|---|---|
| protein kinase | 7 | roscovitine | 7 | roscovitine |
| CDK1/cyclin B | 84 | 70 | nd | nd |
| CDK2/cyclin A | 97 | 94 | nd | nd |
| CDK2/cyclin E | 98 | 95 | 0.04 | 0.22 |
| CDK5/p35 | 95 | 85 | 0.20 | 0.94 |
| CDK7/cyclin H/MAT1 | 96 | 87 | 0.16 | 0.48 |
| CDK9/cyclin T1 | 90 | 87 | 1.00 | 1.77 |
| CK1 | 7 | 1 | nd | nd |
| CK2 | 19 | 10 | nd | nd |
| GSK3A | 32 | 13 | nd | nd |
| GSK3B | 54 | 25 | nd | nd |
| MEK1 | 58 | 38 | nd | nd |
| PRAK | 30 | 28 | nd | nd |
| MSK1 | 39 | 29 | nd | nd |

[a] In the presence of 100 $\mu$M ATP with 10 $\mu$M compound. [b] nd: not determined.

The electron density for the inhibitor is excellent with all its atoms being well-defined in density and allowing the unambiguous positioning of the inhibitor in the binding cleft (Figure 3A). The binding mode of compound 7 in the active site of CDK2 is near identical in the positioning of the pyrazolo[4,3-*d*]pyrimidine core when compared with other homologous ligand structures (Protein Data Bank codes 2A0C, 1G5S, 1W0X, 1CKP, 2A4L, 3DDP, 3NS9) with the pyrazolo[4,3-*d*]pyrimidine being sandwiched between the side chains of Leu134 and Ile10. Similar to other homologous ligand structures, compound 7 forms a conserved hydrogen bond pattern to the backbone carbonyl of Leu83 and to the backbone NH of this same residue. An additional conserved hydrogen bond is found at the backbone carbonyl of Glu81, yet this interaction is considerably shorter when compared to other similar ligand structures (2.77 Å compared to 3.18 Å for the roscovitine complex, PDB code 2A4L) (Figure 3A). Some variation between homologous structures is found in the positioning of the phenyl ring of the benzylamino group. In general this group is sandwiched between the side chain of Ile10 and the backbone of His83. This is also the case with compound 7, although the interaction of the His84 backbone carbonyl at the ortho position of the ring is longer in this structure (Figure 3A). A further difference in the binding mode is apparent when comparing the position of the hydroxymethylpropyl group. This group takes up a similar orientation to that found in the olomoucine II structure (PDB code 2A0C) and is rotated in the opposite direction to that found in the structure containing

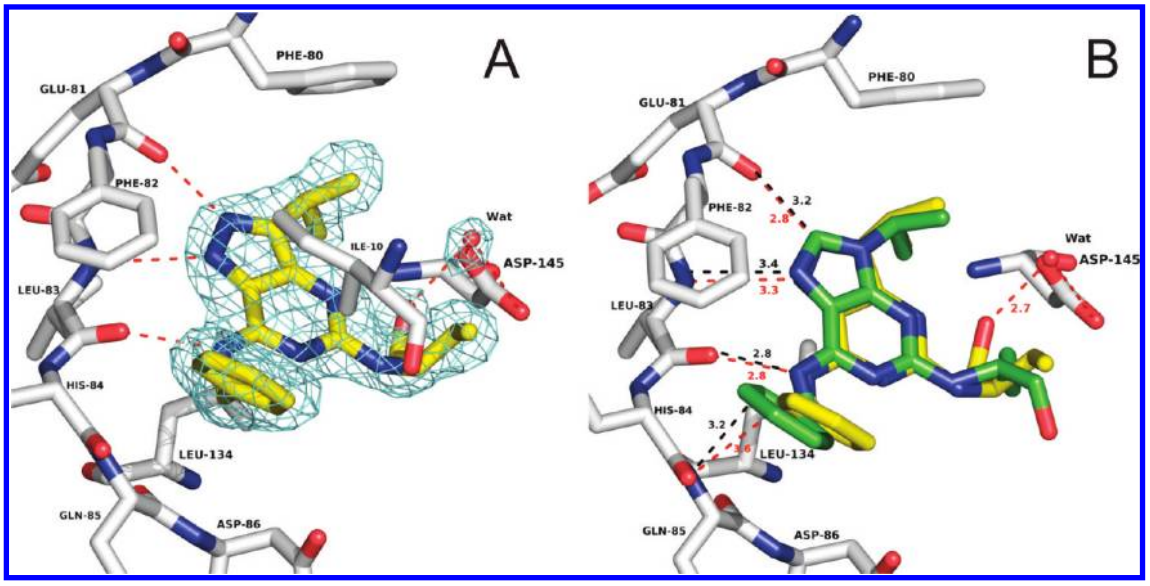


**Figure 3.** (A) Refined electron density for ligand compound **7** within the active site of CDK2. $2|F_o| - |F_c|$ density is colored cyan and is contoured at $1\sigma$ shown around the ligand and an interacting water molecule. Significant protein−ligand interactions are indicated by dashed red lines. (B) Overlay of compound **7** and roscovitine within the active site of CDK2.

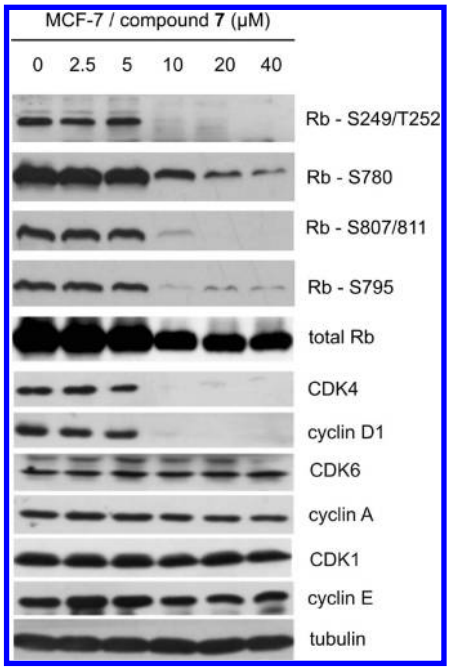


**Figure 4.** Immunoblot analysis of Rb phosphorylation and some cell cycle regulators. Asynchronous MCF-7 cells were exposed for 24 h to the indicated concentrations of compound **7**. Tubulin levels are included as a control for equal protein loading.

roscovitine (PDB code 2A4L, Figure 3B). The hydroxyl atom of this group makes a strong hydrogen bond to a water molecule (water 71), which in turn forms strong interactions to the side chain of Asp145 (Figure 3). This bridging interaction is not observed in any of the homologous ligand/CDK2 complex structures. Therefore, although ligand compound **7** is reminiscent of other roscovitine-like ligands, these are significant differences in their respective binding modes that make compound **7** distinct.

**Cellular Effects of Compound 7.** When exponentially growing human MCF-7 breast cancer cells were treated with compound **7** for 24 h, a dose-dependent inhibition of retinoblastoma protein (Rb) phosphorylation at Ser249/Thr252, Ser807/811, Ser780, and Ser795 became apparent on immunoblots of total cellular proteins probed with phosphospecific antibodies. These results demonstrate the ability of compound **7** to affect the activities of CDK4 and CDK2 in proliferating cells. These CDKs play critical positive roles at the $G_1$/S transition by phosphorylating the Rb protein. Inhibition of cellular CDK activity and consequent Rb dephosphorylation causes cell cycle arrest in the $G_1$ phase. Similar observations have been published not only with roscovitine[53−56] but also with roscovitine isomers imidazo[2,1-*f*]-1,2,4-triazine **13**[25] and pyrazolo-[1,5-*a*]-1,3,5-triazine **7a**.[25]

Moreover, changes of protein abundance for some cell cycle regulators upstream of the Rb protein were monitored in MCF-7 cells treated with compound **7**, compared with mock-treated controls. A significant reduction in CDK4 protein level was observed, and the abundance of cyclin D1, a positive regulator of CDK4, also diminished. In contrast, no changes in protein levels of CDK1, CDK6, and cyclins E and A were seen (Figure 4). This inhibitory pattern, consistent with the cell-cycle effects of compound **7**, was observed in MCF-7 cells also upon treatment with roscovitine[46] and pyrazolo[1,5-*a*]pyrimidine BS-181.[28] On the other hand, human HT-29 colon cancer cells responded to roscovitine treatment by a decrease in cyclin A protein level, while the abundance of CDK4 remained unchanged.[54]

**Cell Cycle Analysis.** The antiproliferative activity of compound **7** was verified by flow cytometry analysis of asynchronously growing MCF-7 cells and the multiple myeloma RPMI-8226 cell line, through double staining with propidium iodide and 5-bromo-2′-deoxyuridine (BrdU). As shown in Figure 5, treatment with both compound **7** and roscovitine arrested the cell cycle progression in the $G_2$/M phase and resulted in decreased S-phase populations in the two cell lines. Upon treatment with higher concentrations of roscovitine and

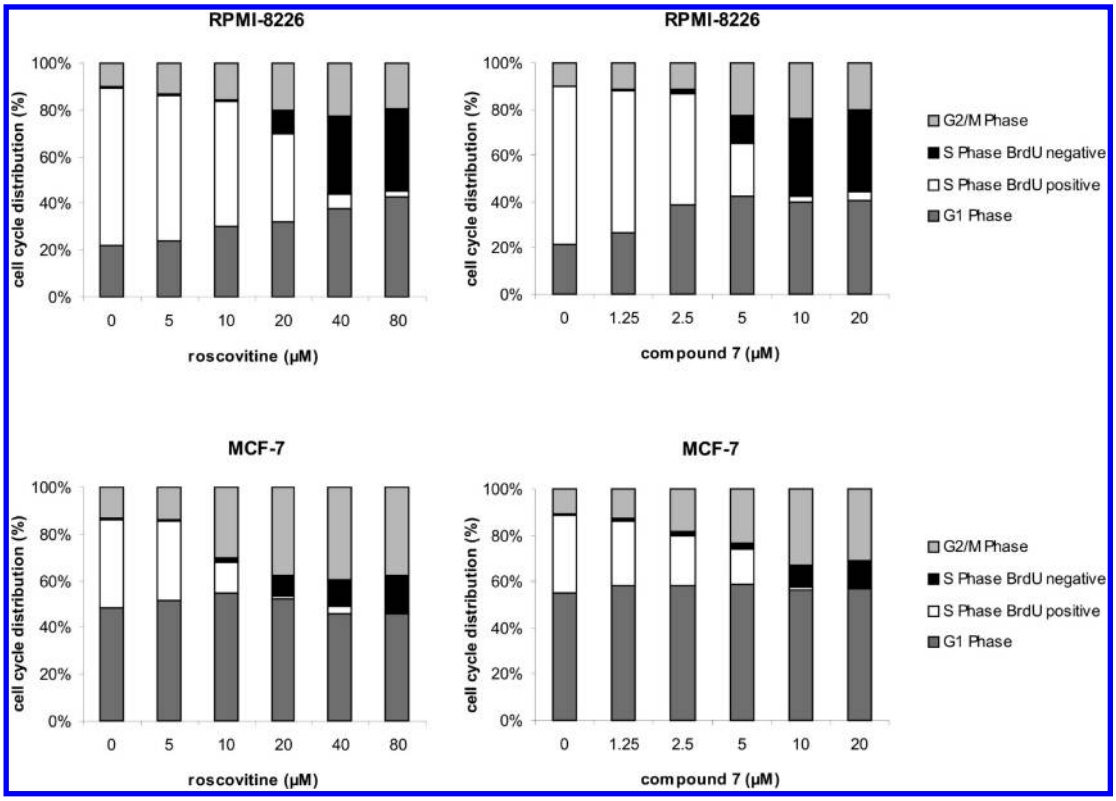


**Figure 5.** Compound 7 arrests cells at various stages of the cell cycle: flow cytometric analysis of BrdU and propidium iodide incorporation in RPMI-8226 and MCF-7 cells treated for 24 h with roscovitine and compound 7, respectively.

compound 7 the populations of cells actively replicating DNA (i.e., BrdU-positive cells) also decreased markedly. In addition, accumulation of RPMI-8226 cells in $G_1$ was found, an outcome not observed in MCF-7 cells. In summary, compound 7 arrested the cell cycle of two human cancer cell lines more efficiently than roscovitine, but both compounds displayed similar patterns of the cell-cycle blockade.

Besides cell cycle changes, increases of $subG_1$ population (indicative of apoptosis) upon treatment with the two compounds were also observed (Figure 5). Notably, compound 7 triggered apoptosis already after 24 h of treatment at compound concentrations above 10 $\mu$M in MCF-7, U266, and RPMI-8226 cells (Figure S3). These results correlate well with data on induction of apoptosis obtained by other apoptotic assays (see below and Figures 6 and S4).

**Induction of Apoptosis.** Most CDK inhibitors, including roscovitine, semisynthetic flavone flavopiridol,[57−59] and 3-substituted indolinone compound SU9516,[60,61] exert a strong proapoptotic effect on multiple myeloma cells through down-regulation of Mcl-1 protein.[53,62−64] Therefore, we studied induction of apoptosis in multiple myeloma cell lines in more detail. Compound 7 induced apoptosis in the multiple myeloma cell line RPMI-8226, as documented by detection of a cleaved fragment of caspase-3 and its enhanced enzymatic activity, by fragmentation of poly(ADP ribose)polymerase 1 (PARP) and by down-regulation of antiapoptotic protein Mcl-1 (Figure 6C). As shown in Figure 6A, treatment with 20 $\mu$M compound 7 induced strong activation of caspases 3 and 7 as quantified by a biochemical assay. This result correlates well not only with the immunoblotting analysis, where the cleavage of caspase-3 zymogene was observed under the same experimental conditions, but also with the flow cytometric detection of the caspase-3 fragment using the anticleaved caspase-3 (Asp175) antibody (Figure 6B,C). Monitoring of the cleavage of PARP, a nuclear target of caspase-3, further confirmed the above results. Taken together, our results clearly showed that compound 7 induces apoptosis in the RPMI-8226 multiple myeloma cell line in a concentration-dependent manner. Furthermore, consistent results were found also for another multiple myeloma cell line, U266 (Figure S5).

**Induction of p53-Dependent Transcription.** Treatment of cells harboring wild-type p53 with CDK inhibitors leads to accumulation of p53 and to an increase of p53-dependent transcription, as shown with roscovitine.[65,66] A strong nuclear immunofluorescence signal of p53 was also evident in MCF-7 cells following treatment with compound 7 (Figure 7A). These results were then confirmed and extended by immunoblotting analyses of the levels of p53 and its targets, $p21^{WAF1}$ and Mdm-2 (Figure 7C). We found that after 24 h incubations of proliferating MCF-7 cells with 20 $\mu$M roscovitine and 10 $\mu$M compound 7 the level of p53 was strongly increased. Moreover, the accumulated p53 was transcriptionally active, as indicated by the enhanced expression of the cell cycle inhibitory protein $p21^{WAF1}$, a well-established transcriptional target of p53.

Next, the effect of compound 7 on p53-dependent transcriptional activity was determined by the $\beta$-galactosidase activity measurement in the human melanoma cell line ARN8.[66] Compound 7 showed a dose-dependent activity effect on p53-regulated transcription, with the maximum impact observed between 10 and 20 $\mu$M (Figure 7B), while the maximal effect of roscovitine was observed at an approximately 1.5-fold higher concentration (data not shown).

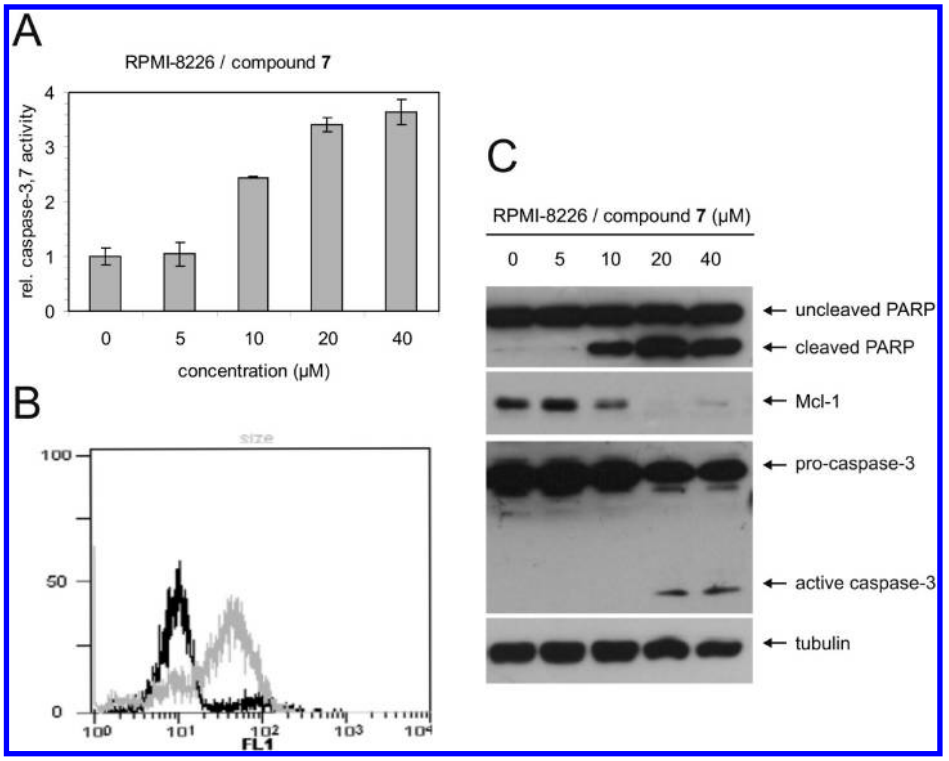


**Figure 6.** Compound 7 induces apoptosis in RPMI-8226 cell line after continuous 24 h treatment. (A) The activities of caspases 3 and 7 measured using a fluorogenic substrate Ac-DEVD-AMC in lysates of cells treated with increasing doses of compound 7. (B) Active fragment of caspase-3 (gray line) detected by flow cytometry using specific anticleaved caspase-3 (Asp175) antibody in cells treated with 20 $\mu$M compound 7. Black and gray lines indicate untreated and treated cells, respectively. (C) Fragmentation of PARP and caspase-3 and down-regulation of Mcl-1 detected by immunoblot analysis. Tubulin levels were monitored to verify equal protein loading.

**Compound 7 Inhibits DNA Repair via Homologous Recombination Independently of RAD51 Protein Abundance.** Homologous recombination (HR) is important for DNA double strand break (DSB) repair, and its proper function is required for the maintenance of genomic stability and cell survival.[67] HR repair seems to be restricted only to S and G2 phases of the cell cycle, where homologous sequences are available, consistent with regulation of HR activity via CDK dependent mechanism(s). Indeed, in yeast, Sae2 protein phosphorylation by CDK was identified as an important HR regulator[68] and a similar CDK-dependent mechanism was proposed also for mammalian cells. However, in mammalian cells the identification of CDK(s) responsible for regulation of HR is rather problematic because studies with roscovitine or flavopiridol also showed rapid down-regulation of a core HR-pathway protein Rad51,[69,70] the effect which may mask any other potential regulatory impact of CDK inhibition on HR. Moreover, Rad51 down-regulation seems unlikely to represent a physiological mode of HR regulation because Rad51 abundance is not markedly altered throughout G1, S, and G2 phases of the cell cycle.[71] Thus, we examined whether compound 7 could be used as an alternative CDK inhibitor, possibly capable of modulating the HR process without affecting the Rad51 status. We selected the highest concentrations of roscovitine, flavopiridol, and compound 7 which do not yet affect the cell cycle progression (Figure S6) and assessed HR using an assay in which HR efficiency to repair DSB within a reporter plasmid in human cells is quantified through measurement of the repair-generated GFP fluorescence signal by flow cytometry.[72] In parallel we monitored the RAD51 protein level by immunoblotting. In cells treated with compound 7 and flavopiridol, the HR efficiency was reduced to 66% and 62% of control values, respectively (Figure 8A). Notably, at the drug concentrations used for the HR assay only flavopiridol caused a significant RAD51 decrease (Figure 8B). Treatment with roscovitine at a concentration not affecting the cell cycle did not influence HR significantly nor did it affect the RAD51 level (Figure 8). On the basis of these results, obtained particularly because of compound 7, we conclude that CDK inhibition can affect HR efficiency independently of effects on RAD51 protein abundance.

## ■ CONCLUSION

Compound 7 was prepared and characterized as a representative of a new group of CDK inhibitors, trisubstituted pyrazolo-[4,3-*d*]pyrimidines. In several biochemical and biological assays, the effects of compound 7 were compared with those of its bioisostere, roscovitine. These analyses showed similar kinase selectivity profiles of roscovitine and compound 7, yet apparently higher efficiency of the latter compound. The overall molecular and cellular effects of compound 7 were consistent with its ability to inhibit CDKs and, furthermore, revealed evidence for a role of CDKs in regulation of DNA repair by HR. The data suggest that blocking HR-mediated repair by compound 7 and perhaps also by other CDK inhibitors could potentially be exploited in cancer therapy in at least three scenarios: (i) to sensitize cancer cells to therapeutically used clastogens including ionizing radiation; (ii) as single agents to affect cancer cells preferentially, because of the tumor-specific oncogene-evoked replication stress and the ensuing constitutive DNA damage[73−75] whose repair requires HR;

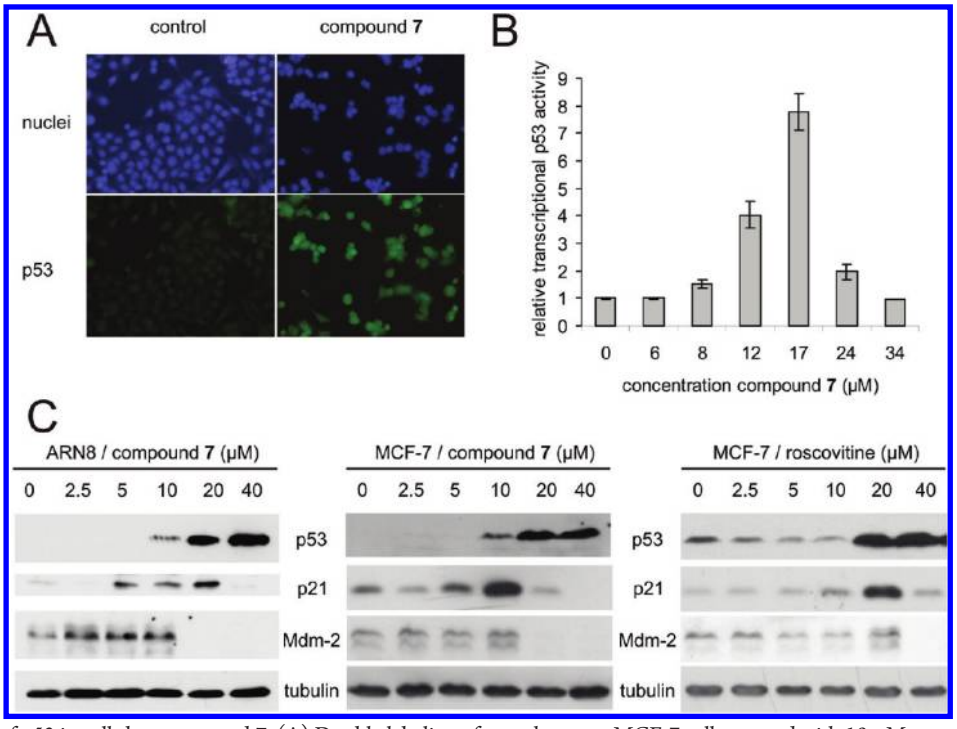


**Figure 7.** Induction of p53 in cells by compound 7. (A) Double labeling of asynchronous MCF-7 cells, treated with 10 $\mu$M compound 7 for 24 h, with anti-p53 antibody and DAPI. (B) Dose-dependent effect of 7 on p53-dependent transcription in ARN8 cells stably transfected with a p53-responsive $\beta$-galactosidase reporter construct and treated with 7 for 24 h. Fluorescence of cleaved product of 4-methylumbelliferon-$\beta$-D-galactopyranoside (MUG) was determined in lysed cells. Results represent the average ± SD for three independent experiments. (C) Immunoblotting analysis of p53 and its targets, $p21^{WAF1}$ and Mdm-2, in MCF-7 or ARN8 cells treated for 24 h with the indicated concentration of compound 7 and roscovitine, respectively. Tubulin is included as controls for equal protein loading.

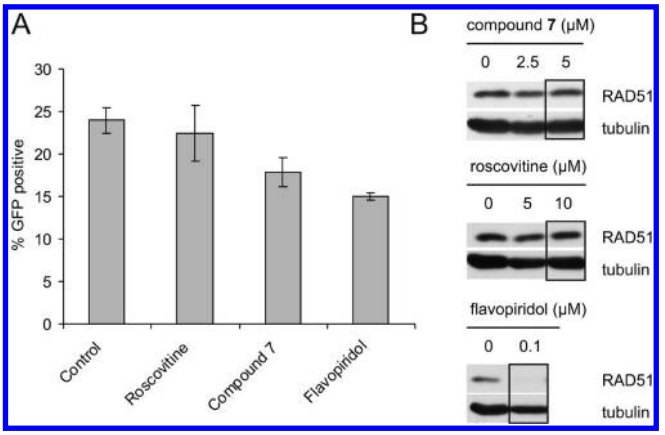


**Figure 8.** Compound 7 reduces homologous recombination. DR-U2OS-GFP cells expressing I-SceI nuclease to produce DSBs within the HR-reporter sequences were used to measure the GFP product as a readout for effects of CDK inhibitors on HR efficiency. (A) GFP level and its fluorescence intensity in DR-U2OS-GFP cells reflect the degree of successful HR-mediated recombination that was subject to modulation by roscovitine (10 $\mu$M), compound 7 (5 $\mu$M), or flavopiridol (0.1 $\mu$M) for 56 h. (B) Protein levels of RAD51 were analyzed by immunoblotting in DR-U2OS-GFP cells exposed to increasing concentrations of the drugs, as indicated. Frames highlight scenarios with drug concentrations used in the HR assay.

(iii) to selectively kill cancer cells that often harbor defects in DNA damage response pathways, taking advantage of the synthetic lethality principle.[67] Altogether, our present characterization of this novel trisubstituted pyrazolo[4,3-*d*]pyrimidine warrants further evaluation of these purine-derived bioisosteres as potential new candidate anticancer drugs.

## EXPERIMENTAL SECTION

**General Experimental Procedures.** Melting points were determined on a Kofler block and are uncorrected. NMR spectra were measured on a Bruker AVANCE III 400 MHz spectrometer (400.13 MHz for $^1$H and 100.61 MHz for $^{13}$C) and a Bruker AVANCE III 600 MHz spectrometer (600.23 MHz for $^1$H and 150.93 MHz for $^{13}$C) and a Varian Geminy 300 (300.1 MHz for $^1$H and 75 MHz for $^{13}$C) in DMSO-$d_6$ or $CDCl_3$ at 303 K. The residual solvent signal was used as an internal standard ($\delta_H$ 2.500 and $\delta_C$ 39.60 for DMSO-$d_6$ or $\delta_H$ 7.265 and $\delta_C$ 77.00 for $CDCl_3$). $^1$H NMR, $^{13}$C NMR, COSY, HSQC, and HMBC results were obtained using standard manufacturers' software (Topspin 2.1, Bruker Biospin GmbH, Rheinstetten Germany). Chemical shifts are given in $\delta$ scale [ppm] and coupling constants in Hz. Digital resolution enabled us to report chemical shifts of protons to 3 and coupling constants to 1 and carbon chemical shifts to 2 decimal places. ESI or APCI mass spectra were determined using a Waters Micromass ZMD mass spectrometer (direct inlet, coin voltage 20 V). IR spectra were recorded on an FT-IR Nicolet 200 instrument with KBr tablet. Compound purity was determined by elemental analyses (0.4%) or LC−MS analysis and was confirmed to be >95% for all compounds. Merck silica gel Kieselgel 60 (230−400 mesh) was used for column chromatography.

**Prepared Compounds.** *4-Amino-5-isopropyl-1(2)H-pyrazole-3-carboxamide (**1**).* **1** was prepared according to the published synthesis.[43]

*3-Isopropyl-5-sulfanyl-1(2)H-pyrazolo[4,3-d]pyrimidin-7-ol (**2**).* A mixture of amide **1** (1.5 g, 9 mmol) and thiourea (3.8 g, 46 mmol) was fused (195 °C) for 30 min under argon atmosphere. After cooling, the reaction melt was suspended in water (20 mL) and the solution was

alkalized at 0 °C by 2 M NaOH solution to pH 12.3. The resulting dark solution was decolorized by carboraffin. The filtered solution was acidified by HCl to pH 5.7−6.0. After 1 h the product was filtered off, washed with cooled water, and dried at 80 °C/20 Torr. Yield 82%, mp >305 °C (dec). MS ESI$^-$: $[M - H]^-$ = 209.3. $^1$H NMR (400 MHz, 303.1 K, DMSO-$d_6$) $\delta$ 1.225 (d, $J$ = 6.9 Hz, 6H, $(CH_3)_2$), 3.370 (sept, $J$ = 6.9 Hz, 1H, CH), 12.116 (br s, 1H), 12.651 (br s, 1H), 13.842 (br s, 1H). $^{13}$C NMR (100 MHz, 303.1 K, DMSO-$d_6$) $\delta$ 21.91 (q, $(CH_3)_2$), 24.08 (d, CH), 124.04 (s), 126.91 (s), 134.08 (s, C-9), 143.13 (s, C-9), 152.57 (s), 155.34 (s). Anal. ($C_8H_{10}N_4OS$) C, H, N, S.

*3-Isopropyl-5-methylsulfanyl-1(2)H-pyrazolo[4,3-d]pyrimidin-7-ol (**3**).* Thiol **2** (16 g, 70 mmol) was added to a mixture of 50 mL of EtOH and 170 mL of water at 35 °C. The pH of the solution was adjusted to 9.3 by adding a water solution of 30% NaOH, and thus, thiol **2** was dissolved. During vigorous agitation dimethylsulfate (6.6 mL, 70 mmol) was added at 20 °C to the reaction mixture. The crystallized product was filtered off, washed (2×) with a mixture of EtOH/$H_2O$ (1/2.5, 20 mL), and water. The product was dried at 80 °C/20 Torr. Yield 90%, mp 213−216 °C. MS ESI$^-$: $[M - H]^-$ = 223.3. $^1$H NMR (600 MHz, 303.1 K, DMSO-$d_6$) $\delta$ 1.349 (d, $J$ = 7.0 Hz, 6H, $(CH_3)_2$), 2.531 (s, 3H, $CH_3S$), 3.216 (sept, $J$ = 7.0 Hz, 1H, CH), 12.398 (s, 1H, NH or OH), 13.513 (s, 1H, NH or OH). $^{13}$C NMR (150 MHz, 303.1 K, DMSO-$d_6$) $\delta$ 12,94 (q, $CH_3S$), 21.69 (q, $(CH_3)_2$), 26.32 (d, CH), 125.08 (s), 136.91 (s, C-4), 149.48 (s, C-9), 151.94 (s, C-2), 153.51 (s). Tautomer: $^1$H NMR (600 MHz, 303.1 K, DMSO-$d_6$) $\delta$ 1.369 (d, $J$ = 7.0 Hz, 6H, $(CH_3)_2$), 2.50* (s, 3H, $CH_3S$), 3.285 (sept, $J$ = 7.0 Hz, 1H, CH), 11.959 (s, 1H, NH or OH), 13.770 (s, 1H, NH or OH). $^{13}$C NMR (150 MHz, 303.1 K, DMSO-$d_6$) $\delta$ 12,86 (q, $CH_3S$), 21.69 (q, $(CH_3)_2$), 24.74 (d, CH), 133.60 (s), 134.69 (s), 140.34 (s, C-9), 151.21 (s, C-2), 157.35 (s). HSQC readout was done.

*7-Chloro-3-isopropyl-5-methylsulfanyl-1(2)H-pyrazolo[4,3-d]pyrimidine (**4**).* Dimethylaniline (30 mL) was dropped under nitrogen atmosphere into a mixture of thioether **3** (18 g, 80 mmol) and $POCl_3$ (120 mL) during 30 min. Then the reaction mixture was refluxed for 5 h (bath temperature of 108 °C). After cooling to room temperature, the reaction mixture was concentrated under vacuum (the excess of $POCl_3$ was removed). Methyl *tert*-butyl ether (MTBE) (140 mL) was added, and during agitation water (50 mL) was added. The organic phase was separated off, and the water phase was extracted once more by MTBE. Combined organic phases were diluted by 70 mL of water and alkalized by solid $NaHCO_3$ (2 g) to pH 7.5. The mixture was then agitated for 2 h. The organic phase was separated by carboraffin trituration and dried by $MgSO_4$. Crystallization from MTBE−heptane afforded (after drying at 70 °C/20 Torr) 16 g of a yellow product. Yield 80%, mp >170 °C (dec). MS ESI$^-$: $[M - H]^-$ = 241.3 (100%), 243 (30%). $^1$H NMR (400 MHz, 303.1 K, $CDCl_3$) $\delta$ 1.500 (d, $J$ = 7.0 Hz, 6H, $(CH_3)_2$), 2.644 (s, 3H, $CH_3S$), 3.488 (sept, $J$ = 7.0 Hz, 1H, CH). $^{13}$C NMR (100 MHz, 303.1 K, $CDCl_3$) $\delta$ 14.59 (q, $CH_3S$), 21.34 (q, $(CH_3)_2$), 27.12 (d, CH), 128.77 (s, C-6), 144.21 (s, C-5), 144.51 (s, C-4), 151.96 (s, C-9), 163.60 (s, C-2). Anal. ($C_9H_{11}ClN_4S$) C, H, N, Cl.

*7-Benzylamino-3-isopropyl-5-methylsulfanyl-1(2)H-pyrazolo[4,3-d]pyrimidine Hydrochloride (**5**).* 7-Chloro derivative (8.5 g, 35 mmol), benzylamine (9 mL, 85 mmol), and triethylamine (23 mL, 230 mmol) in 50 mL of 1-butanol were heated with stirring at 100 °C for 3 h. The solution was evaporated to dryness in vacuum, and the residue was partitioned between $H_2O$ and EtOAc. The combined organic phase was purified by carboraffin and dried with magnesium sulfate and evaporated. Product was dissolved in a mixture of 30 mL of MTBE, 10 mL of $H_2O$, and 4 mL of isopropanol. After acidification by 5 N HCl to pH 0.5, hydrochloride **5** crystallized. Product was filtered off, washed twice with a mixture of MTBE/2-propanol (7/3, 10 mL), and dried at 70 °C/20 Torr. Yield 11 g, 88%, mp 197−204 °C (after recrystallization from boiling EtOH, mp 205−210 °C). MS ESI$^-$: $[M - H]^-$ = 312.3 (100%), 348 (50%, M + Cl$^-$). MS ESI$^+$: 314.3 (100%, M + H$^+$). IR (cm$^{-1}$): 1618,1581,1532, 1353, 1246, 1181, 1062, 924, 698. $^1$H NMR (400 MHz, 303.1 K, $CDCl_3$) $\delta$ 1.340 (d, $J$ = 7.0 Hz, 6H, $(CH_3)_2$), 2.541 (s, 3H, $CH_3S$), 3.300 (sept, $J$ = 7.0 Hz, 1H, CH), 4.762 (br s, 2H, NHC**H**$_2$), 6.658 (br s, 1H, N**H**$CH_2$), 7.213−7.277 (5H, m, H-ortho, H-meta, H-para), 11.615 (br s, H-7 or H-8). $^{13}$C NMR (100 MHz, 303.1 K, $CDCl_3$) $\delta$ 14.42 (q, $CH_3S$), 21.51 (q, $(CH_3)_2$), 26.01 (d, CH), 44.65 (t, $NHCH_2$), 127.53 (d, C-para), 127.79 (d, C-ortho), 128.62 (d, C-meta), 137.96 (s, C-ipso), 138.77 (s), 151.24 (s, C-9), 163.34 (s, C-2). Anal. ($C_{16}H_{19}N_5S$) C, H, N.

*7-Benzylamino-3-isopropyl-5-methylsulfonyl-1(2)H-pyrazolo[4,3-d]pyrimidin (**6**).* Thioether **5** (liberated base, 8 g, 26 mmol) was dissolved in 40 mL of ethanol, and solution of 20 g of Oxone in 50 mL of $H_2O$ was added at 45−50 °C. Oxygenation was checked by TLC (silica gel, MeOH/toluene, 1/9) and was completed in 30 min. Water (130 mL) and ethyl acetate (50 mL) were added. Product was extracted in the organic phase once more with 20 mL of ethyl acetate. The combined organic phase was purified by carboraffin and dried with magnesium sulfate and evaporated. Product was crystallized from methanol. Yield 7.5 g, 83%, mp 96 °C. MS ESI$^-$: $[M - H]^-$ = 344.3 (100%, M − H$^+$). MS ESI$^+$: 346.3 (100%, M + H$^+$). IR (cm$^{-1}$): 1626, 1534, 1453, 1359, 1297, 1128 ($SO_2$), 1060, 926, 753. $^1$H NMR (400 MHz, 303.1 K, $CDCl_3$) $\delta$ 1.325 (d, $J$ = 5.0 Hz, 6H, $(CH_3)_2$), 3.222 (s, 3H, $CH_3SO_2$), 3.349 (br s, 1H, CH), 4.761 (br s, 2H, NHC**H**$_2$), 7.259−7.185 (3H, m, H-meta, H-para), 7.310 (2H, m, H-ortho). $^{13}$C NMR (100 MHz, 303.1 K, $CDCl_3$) $\delta$ 21.56 (q, $(CH_3)_2$), 26.14 (d, CH), 39.13 (q, $CH_3SO_2$), 45.17 (t, N**H**$CH_2$), 124.79 (s), 127.64 (d, C-para), 128.01 (d, C-ortho), 128.64 (d, C-meta), 137.27 (s, C-ipso), 150.68 (s), 151.39 (s), 157.79 (s, C-2). Anal. ($C_{16}H_{19}N_5O_2S$) C, H, N.

*7-Benzylamino-5(R)-[2-(hydroxymethyl)propyl]amino-3-isopropyl-1(2)H-pyrazolo[4,3-d]pyrimidine (**7**).* Methylsulfone **6** (0.2 g, 0.58 mmol) and *R*-(−)-2-amino-1-butanol (2 mL, 23 mmol) were heated in sealed ampule for 3 h to 160 °C. Excess of the amine was evaporated at a temperature below 70 °C, and the residue was partitioned in $CHCl_3$/$H_2O$. The combined organic phases were dried with magnesium sulfate and evaporated. Product was purified by column flash chromatography on silica gel stepwise with 1%, 2%, 4%, and 6% MeOH in $CHCl_3$. Product was obtained in noncrystallizable amorphous colorless glass form. Yield 54 mg, 25%, $[\alpha]_D$ +53 ($c$ 1.35, $CHCl_3$). MS ESI$^+$: $[M + H]^+$ = 355.4 (100). MS ESI$^-$: $[M - H]^-$ = 353.3 (100). $^1$H NMR (300 MHz, DMSO-$d_6$) 0.85 (t, $J$ = 7,5 Hz, 3H, C**H**$_3$CH$_2$), 1.32 (d, $J$ = 7.0 Hz, 6H, (C**H**$_3$)$_2$CH), 1.39−1.68 (m, 2H, C**H**$_2$CH$_3$), 3,16 (sept, $J$ = 7,0 Hz, 1H, C**H**$(CH_3)_2$), 3.37 −3.51 (m, 2H, C**H**$_2$OH), 3.78 (m, 1H, C**H**NH), 4.68 (br s, 2H, $CH_2$Ph), 5.74 (br s, 1H, NH), 7.26 (m, 1H, H-para), 7.34 (m, 2H, H-meta), 7.39 (m, 2H, H-ortho), 11.79 bs ($^1/_2$ H, NH), 13,28 bs ($^1/_2$ H, NH). $^{13}$C NMR (75 MHz, DMSO-$d_6$) $\delta$ 10.6, 21.5, 21.6, 23.8, 25.9, 43.0, 54.2, 63.4, 126.9, 127.5, 128.3, 139.3, 147.1, 157.6 . Anal. ($C_{19}H_{26}N_6O$) C, H, N.

**Enzyme Inhibition Assay.** CDK2/cyclin E kinase was produced in Sf9 insect cells via baculoviral infection and purified on a NiNTA column (Qiagen). CDK5/p35, CDK7cyclin H/MAT1, and CDK9/cyclin T1 were purchased from ProQinase GmbH. The kinase reactions were assayed with 1 mg/mL histone H1 (for CDK2 and CDK5) or $(YSPTSPS)_2KK$ peptide (for CDK7 and CDK9) in the presence of 15/0.15/1.5/1.5 $\mu$M ATP (for CDK2/CDK5/CDK7/CDK9), 0.05 $\mu$Ci [$\gamma$-$^{33}$P]ATP, and the test compound in a final volume of 10 $\mu$L, all in a reaction buffer (60 mM HEPES−NaOH, pH 7.5, 3 mM $MgCl_2$, 3 mM $MnCl_2$, 3 $\mu$M sodium orthovanadate, 1.2 mM DTT, 2.5 $\mu$g/50 $\mu$L $PEG_{20.000}$). The reactions were stopped by adding 5 $\mu$L of 3% aqueous $H_3PO_4$. Aliquots were spotted onto P-81 phosphocellulose (Whatman), washed 3× with 0.5% aqueous $H_3PO_4$, and finally air-dried. Kinase inhibition was quantified using digital image analyzer FLA-7000 (Fujifilm). The concentration of the test compounds required to decrease the CDK by 50% was determined from dose-response curves and designated $IC_{50}$.

**Kinase Selectivity.** All kinase assays were carried out by the SelectScreen Kinase Profiling Service in the presence of 100 $\mu$M ATP and 10 $\mu$M compound and performed according to the standard protocol of Invitrogen.

**Crystallization and Structure Determination.** Human recombinant CDK2 was purchased from ProQinase GmbH, and crystals were grown following the protocol of the supplier. The compound 7/CDK2 complex was prepared by transferring a coverslip containing a drop of native CDK2 crystals over a well solution of 35% PEG 6000 and equilibrating at 17 °C for 24 h. A single crystal of CDK2 was transferred from this drop into a 1 $\mu$L drop of 35% PEG 6000, 100 mM Na HEPES buffer (pH 7.5), 1 mM compound 7, and 5 mM DMSO and placed over a well of the same solution. Crystals were left to soak for 2 days. The crystal of about 0.1 mm in length was mounted in a 0.1−0.2 mm cryoloop (Hampton Research) and was flash-frozen in liquid nitrogen. The soaking solution acted as a cryoprotectant. All diffraction data were collected at 100 K (Cryostream) using a Rigaku Micro7 rotating anode generator and a Mar345 detector (MarResearch). Data processing was carried out using the programs MOSFLM and SCALA.[76] Initial structure solution was performed using the program PHASER[77] using an available CDK2 structure (PDB code 2A0C). The programs REFMAC[78] and PHENIX[79] were used for refinement, with manual refinement and waterfitting being performed by the program COOT.[80] Crystallographic processing and refinement statistics are summarized in Supporting Information (Table S1). Atomic coordinates have been deposited in the Brookhaven Protein Data Bank under the accession code 3PJ8.

**Cell Maintenance and Cytotoxicity Assay.** The cytotoxicity of the studied compounds was determined with cell lines of different histological origin. The cells, cultured in DMEM (supplemented with 10% fetal calf serum, 4 mM glutamine, 100 IU/mL penicillin, 100 $\mu$g/mL streptomycin) in a humidified $CO_2$ incubator at 37 °C, were redistributed into 96-well microtiter plates at appropriate densities for their respective cell sizes and growth rates. After preincubation, test compounds in 3-fold dilutions were added in triplicates. Treatment lasted for 72 h and then calcein AM solution was added. The fluorescence of the live cells was measured at 485 nm/538 nm (excitation/emission) with a Fluoroskan Ascent microplate reader (Labsystems). $IC_{50}$ values, the drug concentrations reducing number of viable cells to 50%, were determined from the dose-response curves.

**Immunoblotting.** For direct immunoblotting, total cellular protein lysates were prepared by harvesting treated cells in Laemmli sample buffer. Proteins were separated on SDS-polyacrylamide gels and electroblotted onto nitrocellulose membrane. The blotted membranes were stained with 0.2% Ponceau-S in 1% aqueous acetic acid to verify equal protein loading, destained, and blocked in PBS and 0.1% Tween 20 (PBS-T) with 5% low fat milk or 3% bovine serum albumin (BSA). The membranes were then incubated with specific antibodies overnight at 4 °C. After being washed three times in PBS-T, the membranes were incubated with a 1:2000 dilution of peroxidase-conjugated secondary antibodies. After another three washes in PBS-T, peroxidase activity was detected using ECL+ reagents (AP Biotech) according to the manufacturer's instructions.

**Antibodies.** Specific antibodies were purchased from Cell Signaling Technology (antitotal pRb, clone 4H1, and anti-pRb antibodies phosphorylated at S780, S795, and S807/811), Sigma-Aldrich (anti-pRb phosphorylated at Ser249/Thr252, anti-α-tubulin, clone DM1A, peroxidase-labeled secondary antibodies), Santa Cruz Biotechnology (anti-Mcl-1, clone S-19, anti-PARP, clone F-2, anti-Mdm-2, clone SMP14, anti-RAD51, clone H-92, anti CDK1, clone B-6; anti-cyclin E, clone HE12), DAKO Cytomation (anti-caspase-3), Roche Applied Science (anti-5-bromo-2′-deoxyuridine-fluorescein, clone BMC 9318), Jackson ImmunoResearch Laboratory (fluorescein-conjugated Goat Anti-Mouse IgG), Beckman Coulter (anti-cleaved caspase-3) or were a generous gift from Dr. B. Vojtěšek (anti-p53, clone DO-1, anti-$p21^{WAF1}$, clone 118, anti-CDK4, anti-cyclin D1, anti-CDK6, anti-cyclin A).

**BrdU Incorporation and Cell Cycle Analysis.** Subconfluent MCF-7 cells were treated with compound 7 or roscovitine at different concentrations for 24 h. The cultures were fed and pulse-labeled with 10 $\mu$M 5-bromo-2′-deoxyuridine (BrdU) for 30 min at 37 °C before harvesting. The cells were trypsinized, washed by PBS containing 1% BSA (PBS/BSA), fixed with ice-cold 70% ethanol, incubated on ice for 30 min, washed with PBS/BSA again, and resuspended in 2 M HCl for 30 min at room temperature in order to denature their DNA. Following neutralization with 0.1 M $Na_2B_4O_7$, the cells were harvested by centrifugation and washed with PBS/BSA containing 0.5% Tween-20. They were then stained with anti-BrdU fluorescein-labeled antibody (1:50) for 30 min at room temperature in the dark. The cells were then washed with PBS, incubated with propidium iodide (0.1 mg/mL) and RNase A (0.5 mg/mL) for 1 h at room temperature in the dark and finally analyzed by flow cytometry using a 488 nm laser (Cell Lab Quanta SC, Beckman Coulter).

**p53-Dependent Transcriptional Activity.** To measure p53-dependent transcriptional activity, $\beta$-galactosidase activity was determined in the human melanoma cell line ARN-8, stably transfected with a p53-responsive reporter construct pRGCΔfoslacZ.[66] After 24 h of incubation with the inhibitors the cells were permeabilized with 0.3% Triton X-100 for 15 min, and then 4-methylumbelliferon-$\beta$-D-galactopyranoside was added as a substrate to a final concentration of 80 $\mu$M. After 1 h the fluorescence was measured at 355 nm/460 nm (excitation/emission) with a Fluoroskan Ascent microplate reader (Labsystems).

**Immunofluorescence.** MCF-7 cells grown on coverslips were treated with increasing concentrations of compounds for 24 h. Slips were then rinsed in PBS, and cells were fixed in methanol/acetone (1:1) at −20 °C for at least 1 h. The coverslips were then rehydrated in PBS for 10−20 min, rinsed with 10% fetal bovine serum, and incubated with the mouse monoclonal anti-p53 antibody (DO-1) for 1 h at room temperature. The samples were then washed three times with PBS before being incubated for 1 h with a secondary fluorescein isothiocyanate-conjugated anti-mouse IgG antibody. After incubation the coverslips were rinsed three times in PBS and then the nuclei were stained by DAPI (MP Biomedicals). After the final wash by water the coverslips were mounted on microscope slides using Mowiol mounting medium (Calbiochem) and observed using a fluorescence microscope (Olympus BX50) coupled with a digital camera (Olympus DP71).

**Caspase-3/7 Assay.** The cells were harvested by centrifugation and homogenized in an extraction buffer (10 mM KCl, 5 mM HEPES, 1 mM EDTA, 1 mM EGTA, 0.2% CHAPS, inhibitors of proteases, pH 7.4) on ice for 20 min. The homogenates were clarified by centrifugation at 10000*g* for 30 min at 4 °C. The proteins were quantified by the Bradford method and diluted to equal concentrations. Lysates were then incubated for 1 h with 100 $\mu$M Ac-DEVD-AMC as substrate in the assay buffer (25 mM PIPES, 2 mM EGTA, 2 mM $MgCl_2$, 5 mM DTT, pH 7.3). For negative controls, the lysates were supplemented with 100 $\mu$M Ac-DEVD-CHO as a caspase-3/7 inhibitor. The fluorescence of the product was measured using a Fluoroskan Ascent microplate reader (Labsystems) at 355 nm /460 nm (excitation/emission).

**Flow Cytometry Analysis of Cleaved Caspase-3.** RPMI-8226 cells were collected by centrifugation, and the pellets were resuspended in 4% formaldehyde solution for 10 min at 37 °C. The cells were then permeabilized by adding ice-cold methanol to a final concentration of 90% and incubated for 30 min on ice. Subsequently the cells were rinsed in BSA/PBS, pelleted, resuspended in a few drops of BSA/PBS, and incubated for 10 min at room temperature. Then anticleaved caspase-3 antibody conjugated with Alexa Fluor 488 (Beckman Coulter) was added, and the cells were incubated for 1 h in the dark at room temperature. Finally the cells were washed in BSA/PBS, resuspended

again, and analyzed by flow cytometry using a 488 nm laser (Cell Lab Quanta SC, Beckman Coulter).

**Homologous Recombination Assay.** A U2OS clone containing a single complete copy of the integrated HR reporter hprt-DR-GFP was obtained from Pierce et al.[81] DR-U2OS-GFP cells ($3.3 \times 10^5$ per well) were seeded in 100 mm dishes and transfected with 1 $\mu$g of pCKA-I-SceI plasmid using Fugene 6 reagent. Sixteen hours later, the medium was replaced with fresh medium containing tested compounds (5 $\mu$M for compound **7**, 10 $\mu$M for roscovitine, 0.1 $\mu$M for flavopiridol). Cells were harvested after 2 days for flow cytometric analysis on a Cell Lab Quanta SC cytometer (Beckman Coulter).

**NCI60 Cytotoxicity Assay.** Tests of toxicity on NCI60, a set of 59 human cancer cell lines derived from nine tissue types, were performed at the Developmental Therapeutics Program of the National Cancer Institute (Bethesda, MD, U.S.). The cytotoxicity of compound **7** was evaluated by measuring total cell protein using the sulforhodamine B method according to the standard protocol at time 0 and after 48 h. The highest concentration tested was 100 $\mu$M. $GI_{50}$, TGI, and $LC_{50}$ (concentration of a drug inducing 50% reduction of growth, total growth inhibition, and 50% reduction of initial cell population, respectively) were estimated from the dose-response curves.

**Correlation Analysis of NCI60 Activity.** The activity pattern ($GI_{50}$ values for individual NCI60 cell lines) of compound **7** was correlated with the drug activity patterns in the DTP cancer screening data set, May 2009 release (http://dtp.nci.nih.gov/docs/cancer/cancer_data.html). Pearson correlation coefficients ($r$) were calculated on a log−log scale. Signed version of coefficient of determination is defined as $[r/\mathrm{abs}(r)]r^2$. Only the activity patterns fulfilling following criteria were analyzed: (1) $GI_{50}$ values for at least 50 cell lines, (2) $GI_{50}$ reached against more than 50% of the cell lines tested, and (3) $GI_{50}$ for the most sensitive cell line at least 5 times lower than $GI_{50}$ for the most resistant cell line. Experimentally validated low molecular inhibitors of CDKs 1, 2, 4, 5, 7, 8, 9 and glycogen synthase kinase-3$\beta$ with $IC_{50} < 100$ $\mu$M were extracted from BindingDB.[51,52] SDfile with the data was downloaded on November 17, 2009. Pubchem ID was used for conversion of BindingDB and NCI60 identifiers. Data manipulation and analysis was done in R 2.8.1.

## ■ ASSOCIATED CONTENT

**Ⓢ Supporting Information.** Crystallographic data collection and refinement statistics, kinase inhibition curves, NCI60 screening of compound **7**, cell cycle analysis of K562, U266, and DR-U2OS-GFP cells upon treatment with roscovitine, compound **7**, and flavopiridol, and the influence of compound **7** on subG1 cell population in different cell lines. This material is available free of charge via the Internet at http://pubs.acs.org.

### Accession Codes

[†]PDB code 3PJ8.

## ■ AUTHOR INFORMATION

### Corresponding Author

*Phone: +420585634854. Fax: +420585634870. E-mail: vladimir.krystof@upol.cz.

## ■ ACKNOWLEDGMENT

The authors thank J. Hudcová and D. Parobková for their technical assistance. Dr. B. Vojtěšek is acknowledged for the gift of antibodies. This work was supported by GACR Grants 204/08/511, 301/11/P554, and 301/02/0475, GAAV Grant IAA50-1370902, IGAMZ Grants NS10282-3/2009 and NT/11065-5/2010, the European Commission (Projects Infla-Care and CZ.1.05/2.1.00/01.0030), and Grant MSM6198959216 and Grant ED0007/01/01 of Centre of the Region Haná for Biotechnological and Agricultural Research. Cytotoxicity testing on NCI60 panel was done at the Developmental Therapeutics Program (DTP) of the National Cancer Institute (Bethesda, MD, U.S.).

## ■ ABBREVIATIONS USED

BrdU, 5-bromo-2′-deoxyuridine; CDK, cyclin-dependent kinase; CK, casein kinase; DSB, double strand breaks; SAR, structure−activity relationship; $GI_{50}$, growth inhibition 50%; GSK, glycogen synthase kinase; HR, homologous recombination; $LC_{50}$, reduction of initial cell population 50%; MEK1, MAPK/ERK kinase 1; MNK-1, MAPK-interacting kinase 1; MSK, mitogen- and stress-activated protein kinase; MTBE, methyl *tert*-butyl ether; MUG, 4-methylumbelliferon-$\beta$-D-galactopyranoside; NCI, National Cancer Institute; PARP, poly(ADP ribose)polymerase 1; PCNA, proliferating cell nuclear antigen; PDB, Protein Data Bank; PRAK, p38-regulated-activated protein kinase; Rb, retinoblastoma protein; TGI, total growth inhibition

## ■ REFERENCES

(1) Malumbres, M.; Carnero, A. Cell cycle deregulation: a common motif in cancer. *Prog. Cell Cycle Res.* **2003**, *5*, 5–18.

(2) Malumbres, M.; Barbacid, M. Cell cycle, CDKs and cancer: a changing paradigm. *Nat. Rev. Cancer* **2009**, *9*, 153–166.

(3) Knockaert, M.; Greengard, P.; Meijer, L. Pharmacological inhibitors of cyclin-dependent kinases. *Trends Pharmacol. Sci.* **2002**, *23*, 417–425.

(4) Malumbres, M.; Barbacid, M. Mammalian cyclin-dependent kinases. *Trends Biochem. Sci.* **2005**, *30*, 630–641.

(5) Krystof, V.; Uldrijan, S. Cyclin-dependent kinase inhibitors as anticancer drugs. *Curr. Drug Targets* **2010**, *11*, 291–302.

(6) Lapenna, S.; Giordano, A. Cell cycle kinases as therapeutic targets for cancer. *Nat. Rev. Drug Discovery* **2009**, *8*, 547–566.

(7) Krystof, V.; Chamrad, I.; Jorda, R.; Kohoutek, J. Pharmacological targeting of CDK9 in cardiac hypertrophy. *Med. Res. Rev.* **2010**, *30*, 646–666.

(8) Leitch, A. E.; Haslett, C.; Rossi, A. G. Cyclin-dependent kinase inhibitor drugs as potential novel anti-inflammatory and pro-resolution agents. *Br. J. Pharmacol.* **2009**, *158*, 1004–1016.

(9) Rossi, A. G.; Sawatzky, D. A.; Walker, A.; Ward, C.; Sheldrake, T. A.; Riley, N. A.; Caldicott, A.; Martinez-Losa, M.; Walker, T. R.; Duffin, R.; Gray, M.; Crescenzi, E.; Martin, M. C.; Brady, H. J.; Savill, J. S.; Dransfield, I.; Haslett, C. Cyclin-dependent kinase inhibitors enhance the resolution of inflammation by promoting inflammatory cell apoptosis. *Nat. Med.* **2006**, *12*, 1056–1064.

(10) Wang, S.; Fischer, P. M. Cyclin-dependent kinase 9: a key transcriptional regulator and potential drug target in oncology, virology and cardiology. *Trends Pharmacol. Sci.* **2008**, *29*, 302–313.

(11) Vesely, J.; Havlicek, L.; Strnad, M.; Blow, J. J.; Donella-Deana, A.; Pinna, L.; Letham, D. S.; Kato, J.; Detivaud, L.; LeClerc, S. Inhibition of cyclin-dependent kinases by purine analogues. *Eur. J. Biochem.* **1994**, *224*, 771–786.

(12) Havlicek, L.; Hanus, J.; Vesely, J.; LeClerc, S.; Meijer, L.; Shaw, G.; Strnad, M. Cytokinin-derived cyclin-dependent kinase inhibitors: synthesis and cdc2 inhibitory activity of olomoucine and related compounds. *J. Med. Chem.* **1997**, *40*, 408–412.

(13) Meijer, L.; Borgne, A.; Mulner, O.; Chong, J. P.; Blow, J. J.; Inagaki, N.; Inagaki, M.; Delcros, J. G.; Moulinoux, J. P. Biochemical and cellular effects of roscovitine, a potent and selective inhibitor of the cyclin-dependent kinases cdc2, cdk2 and cdk5. *Eur. J. Biochem.* **1997**, *243*, 527–536.

(14) Meijer, L.; Bettayeb, K.; Galons, H. (*R*)-Roscovitine (CYC202, Seliciclib). In *Inhibitors of Cyclin-Dependent Kinases as Anti-Tumor Agents*; Smith, P. J., Yue, E. W., Eds.; CRC Press: Boca Raton, FL, 2006; pp 187−226.

(15) Bettayeb, K.; Oumata, N.; Echalier, A.; Ferandin, Y.; Endicott, J. A.; Galons, H.; Meijer, L. CR8, a potent and selective, roscovitine-derived inhibitor of cyclin-dependent kinases. *Oncogene* **2008**, *27*, 5797–5807.

(16) Chang, Y. T.; Gray, N. S.; Rosania, G. R.; Sutherlin, D. P.; Kwon, S.; Norman, T. C.; Sarohia, R.; Leost, M.; Meijer, L.; Schultz, P. G. Synthesis and application of functionally diverse 2,6,9-trisubstituted purine libraries as CDK inhibitors. *Chem. Biol.* **1999**, *6*, 361–375.

(17) Gray, N. S.; Wodicka, L.; Thunnissen, A. M.; Norman, T. C.; Kwon, S.; Espinoza, F. H.; Morgan, D. O.; Barnes, G.; LeClerc, S.; Meijer, L.; Kim, S. H.; Lockhart, D. J.; Schultz, P. G. Exploiting chemical libraries, structure, and genomics in the search for kinase inhibitors. *Science* **1998**, *281*, 533–538.

(18) Krystof, V.; McNae, I. W.; Walkinshaw, M. D.; Fischer, P. M.; Muller, P.; Vojtesek, B.; Orsag, M.; Havlicek, L.; Strnad, M. Antiproliferative activity of olomoucine II, a novel 2,6,9-trisubstituted purine cyclin-dependent kinase inhibitor. *Cell. Mol. Life Sci.* **2005**, *62*, 1763–1771.

(19) Moravec, J.; Krystof, V.; Hanus, J.; Havlicek, L.; Moravcova, D.; Fuksova, K.; Kuzma, M.; Lenobel, R.; Otyepka, M.; Strnad, M. 2,6,8,9-Tetrasubstituted purines as new CDK1 inhibitors. *Bioorg. Med. Chem. Lett.* **2003**, *13*, 2993–2996.

(20) Oumata, N.; Bettayeb, K.; Ferandin, Y.; Demange, L.; Lopez-Giral, A.; Goddard, M. L.; Myrianthopoulos, V.; Mikros, E.; Flajolet, M.; Greengard, P.; Meijer, L.; Galons, H. Roscovitine-derived, dual-specificity inhibitors of cyclin-dependent kinases and casein kinases 1. *J. Med. Chem.* **2008**, *51*, 5229–5242.

(21) Trova, M. P.; Barnes, K. D.; Alicea, L.; Benanti, T.; Bielaska, M.; Bilotta, J.; Bliss, B.; Duong, T. N.; Haydar, S.; Herr, R. J.; Hui, Y.; Johnson, M.; Lehman, J. M.; Peace, D.; Rainka, M.; Snider, P.; Salamone, S.; Tregay, S.; Zheng, X.; Friedrich, T. D. Heterobiaryl purine derivatives as potent antiproliferative agents: inhibitors of cyclin dependent kinases. Part II. *Bioorg. Med. Chem. Lett.* **2009**, *19*, 6613–6617.

(22) Trova, M. P.; Barnes, K. D.; Barford, C.; Benanti, T.; Bielaska, M.; Burry, L.; Lehman, J. M.; Murphy, C.; O'Grady, H.; Peace, D.; Salamone, S.; Smith, J.; Snider, P.; Toporowski, J.; Tregay, S.; Wilson, A.; Wyle, M.; Zheng, X.; Friedrich, T. D. Biaryl purine derivatives as potent antiproliferative agents: inhibitors of cyclin dependent kinases. Part I. *Bioorg. Med. Chem. Lett.* **2009**, *19*, 6608–6612.

(23) Kim, D. C.; Lee, Y. R.; Yang, B. S.; Shin, K. J.; Kim, D. J.; Chung, B. Y.; Yoo, K. H. Synthesis and biological evaluations of pyrazolo[3,4-*d*]pyrimidines as cyclin-dependent kinase 2 inhibitors. *Eur. J. Med. Chem.* **2003**, *38*, 525–532.

(24) Zask, A.; Verheijen, J. C.; Curran, K.; Kaplan, J.; Richard, D. J.; Nowak, P.; Malwitz, D. J.; Brooijmans, N.; Bard, J.; Svenson, K.; Lucas, J.; Toral-Barza, L.; Zhang, W. G.; Hollander, I.; Gibbons, J. J.; Abraham, R. T.; Ayral-Kaloustian, S.; Mansour, T. S.; Yu, K. ATP-competitive inhibitors of the mammalian target of rapamycin: design and synthesis of highly potent and selective pyrazolopyrimidines. *J. Med. Chem.* **2009**, *52*, 5013–5016.

(25) Bettayeb, K.; Sallam, H.; Ferandin, Y.; Popowycz, F.; Fournet, G.; Hassan, M.; Echalier, A.; Bernard, P.; Endicott, J.; Joseph, B.; Meijer, L. N-&-N, a new class of cell death-inducing kinase inhibitors derived from the purine roscovitine. *Mol. Cancer Ther.* **2008**, *7*, 2713–2724.

(26) Popowycz, F.; Fournet, G.; Schneider, C.; Bettayeb, K.; Ferandin, Y.; Lamigeon, C.; Tirado, O. M.; Mateo-Lozano, S.; Notario, V.; Colas, P.; Bernard, P.; Meijer, L.; Joseph, B. Pyrazolo[1,5-*a*]-1,3,5-triazine as a purine bioisostere: access to potent cyclin-dependent kinase inhibitor (*R*)-roscovitine analogue. *J. Med. Chem.* **2009**, *52*, 655–663.

(27) Guzi, T. J. Paruch, K. Pyrazolotriazines as Kinase Inhibitors. Patent WO 2005/082908, 2005.

(28) Ali, S.; Heathcote, D. A.; Kroll, S. H.; Jogalekar, A. S.; Scheiper, B.; Patel, H.; Brackow, J.; Siwicka, A.; Fuchter, M. J.; Periyasamy, M.; Tolhurst, R. S.; Kanneganti, S. K.; Snyder, J. P.; Liotta, D. C.; Aboagye, E. O.; Barrett, A. G.; Coombes, R. C. The development of a selective cyclin-dependent kinase inhibitor that shows antitumor activity. *Cancer Res.* **2009**, *69*, 6208–6215.

(29) Chen, F. X.; Keertikar, K.; Kuo, S; Lee, S.; Raghavan, R. R.; Wu, G. G.; Xie, J. Process and Intermediates for the Synthesis of (3-Alkyl-5-piperidin-1-yl-3,3a-dihydropyrazolo[1,5-*a*]-pyrimidin-7-yl)-amino Derivatives and Intermediates. Patent WO 2008/027220, 2008.

(30) Heathcote, D. A.; Patel, H.; Kroll, S. H.; Hazel, P.; Periyasamy, M.; Alikian, M.; Kanneganti, S. K.; Jogalekar, A. S.; Scheiper, B.; Barbazanges, M.; Blum, A.; Brackow, J.; Siwicka, A.; Pace, R. D.; Fuchter, M. J.; Snyder, J. P.; Liotta, D. C.; Freemont, P. S.; Aboagye, E. O.; Coombes, R. C.; Barrett, A. G.; Ali, S. A novel pyrazolo[1,5-*a*]pyrimidine is a potent inhibitor of cyclin-dependent protein kinases 1, 2, and 9, which demonstrates antitumor effects in human tumor xenografts following oral administration. *J. Med. Chem.* **2010**, *53*, 8508–8522.

(31) Parratt, M. J.; Bower, J. F.; Williams, J. W.; Cansfield, A. D. Pyrazolopyrimidine Compounds and Their Use in Medicine. Patent WO 2004/087707, 2004.

(32) Paruch, K.; Dwyer, M. P.; Alvarez, C.; Brown, C.; Chan, T. Y.; Doll, R. J.; Keertikar, K.; Knutson, C.; McKittrick, B.; Rivera, J.; Rossman, R.; Tucker, G.; Fischmann, T. O.; Hruza, A.; Madison, V.; Nomeir, A. A.; Wang, Y.; Lees, E.; Parry, D.; Sgambellone, N.; Seghezzi, W.; Schultz, L.; Shanahan, F.; Wiswell, D.; Xu, X.; Zhou, Q.; James, R. A.; Paradkar, V. M.; Park, H.; Rokosz, L. R.; Stauffer, T. M.; Guzi, T. J. Pyrazolo[1,5-*a*]pyrimidines as orally available inhibitors of cyclin-dependent kinase 2. *Bioorg. Med. Chem. Lett.* **2007**, *17*, 6220–6223.

(33) Snyder, J. P.; Liotta, D. C.; Barrett, A. G.; Coombes, R. C.; Ali, S.; Siwicka, A.; Brackow, J.; Scheiper, B. Selective Inhibitors for Cyclin-Dependent Kinases. Patent WO 2008/151304, 2008.

(34) Williamson, D. S.; Parratt, M. J.; Bower, J. F.; Moore, J. D.; Richardson, C. M.; Dokurno, P.; Cansfield, A. D.; Francis, G. L.; Hebdon, R. J.; Howes, R.; Jackson, P. S.; Lockie, A. M.; Murray, J. B.; Nunns, C. L.; Powles, J.; Robertson, A.; Surgenor, A. E.; Torrance, C. J. Structure-guided design of pyrazolo[1,5-*a*]pyrimidines as inhibitors of human cyclin-dependent kinase 2. *Bioorg. Med. Chem. Lett.* **2005**, *15*, 863–867.

(35) Paruch, K.; Guzi, T. J.; Dwyer, D. M.; Doll, R. J.; Girijavallabhan, V. M.; Mallams, A. K. Imidazopyrazines as Cyclin Dependent Kinase Inhibitors. Patent WO 2004/026877, 2004.

(36) Yu, T.; Belanger, D. B.; Kerekes, A. D.; Meng, Z.; Tagat, J. R.; Espozite, S. J.; Mandal, A. K.; Xiao, Y.; Kulkarni, B. A.; Zhang, Y.; Curran, P. J.; Doll, R.; Sidiqui, M. A. Imidazopyrazines as Protein Kinase Inhibitors. Patent WO 2008/156614, 2008.

(37) Richardson, C. M.; Williamson, D. S.; Parratt, M. J.; Borgognoni, J.; Cansfield, A. D.; Dokurno, P.; Francis, G. L.; Howes, R.; Moore, J. D.; Murray, J. B.; Robertson, A.; Surgenor, A. E.; Torrance, C. J. Triazolo[1,5-*a*]pyrimidines as novel CDK2 inhibitors: protein structure-guided design and SAR. *Bioorg. Med. Chem. Lett.* **2006**, *16*, 1353–1357.

(38) Bower, J. F.; Cansfield, A.; Jordan, A.; Parrat, M.; WAlmsley, L.; Williamson, D. Triazolo[1,5-*a*]pyrimidines and Their Use in Medicine. Patent WO 2004/108136, 2004.

(39) Meijer, L.; Bettayeb, K.; Galons, H.; Demange, L.; Oumata, N. Perharidines as CDK Inhibitors. Patent WO 2009/034411, 2009.

(40) Capek, P.; Otmar, M.; Masojidkova, M.; Votruba, I.; Holy, A. A facile synthesis of 9-deaza analogue of olomoucine. *Collect. Czech. Chem. Commun.* **2003**, *68*, 779–791.

(41) Moravcova, D.; Krystof, V.; Havlicek, L.; Moravec, J.; Lenobel, R.; Strnad, M. Pyrazolo[4,3-*d*]pyrimidines as new generation of cyclin-dependent kinase inhibitors. *Bioorg. Med. Chem. Lett.* **2003**, *13*, 2989–2992.

(42) Havlicek, L.; Fuksova, K.; Krystof, V.; Orsag, M.; Vojtesek, B.; Strnad, M. 8-Azapurines as new inhibitors of cyclin-dependent kinases. *Bioorg. Med. Chem.* **2005**, *13*, 5399–5407.

(43) Krystof, V.; Moravcova, D.; Paprskarova, M.; Barbier, P.; Peyrot, V.; Hlobilkova, A.; Havlicek, L.; Strnad, M. Synthesis and biological activity of 8-azapurine and pyrazolo[4,3-*d*]pyrimidine analogues of myoseverin. *Eur. J. Med. Chem.* **2006**, *41*, 1405–1411.

(44) Shoemaker, R. H. The NCI60 human tumour cell line anticancer drug screen. *Nat. Rev. Cancer* **2006**, *6*, 813–823.

(45) McClue, S. J.; Blake, D.; Clarke, R.; Cowan, A.; Cummings, L.; Fischer, P. M.; MacKenzie, M.; Melville, J.; Stewart, K.; Wang, S.; Zhelev, N.; Zheleva, D.; Lane, D. P. In vitro and in vivo antitumor properties of the cyclin dependent kinase inhibitor CYC202 (*R*-roscovitine). *Int. J. Cancer* **2002**, *102*, 463–468.

(46) Paprskarova, M.; Krystof, V.; Jorda, R.; Dzubak, P.; Hajduch, M.; Wesierska-Gadek, J.; Strnad, M. Functional p53 in cells contributes to the anticancer effect of the cyclin-dependent kinase inhibitor roscovitine. *J. Cell. Biochem.* **2009**, *107*, 428–437.

(47) Payton, M.; Chung, G.; Yakowec, P.; Wong, A.; Powers, D.; Xiong, L.; Zhang, N.; Leal, J.; Bush, T. L.; Santora, V.; Askew, B.; Tasker, A.; Radinsky, R.; Kendall, R.; Coats, S. Discovery and evaluation of dual CDK1 and CDK2 inhibitors. *Cancer Res.* **2006**, *66*, 4299–4308.

(48) Knauf, U.; Tschopp, C.; Gram, H. Negative regulation of protein translation by mitogen-activated protein kinase-interacting kinases 1 and 2. *Mol. Cell. Biol.* **2001**, *21*, 5500–5511.

(49) Topisirovic, I.; Ruiz-Gutierrez, M.; Borden, K. L. Phosphorylation of the eukaryotic translation initiation factor eIF4E contributes to its transformation and mRNA transport activities. *Cancer Res.* **2004**, *64*, 8639–8642.

(50) Culjkovic, B.; Topisirovic, I.; Skrabanek, L.; Ruiz-Gutierrez, M.; Borden, K. L. eIF4E promotes nuclear export of cyclin D1 mRNAs via an element in the 3′UTR. *J. Cell Biol.* **2005**, *169*, 245–256.

(51) Chen, X.; Lin, Y.; Liu, M.; Gilson, M. K. The binding database: data management and interface design. *Bioinformatics* **2002**, *18*, 130–139.

(52) Liu, T.; Lin, Y.; Wen, X.; Jorissen, R. N.; Gilson, M. K. BindingDB: a Web-accessible database of experimentally determined protein−ligand binding affinities. *Nucleic Acids Res.* **2007**, *35*, D198–D201.

(53) MacCallum, D. E.; Melville, J.; Frame, S.; Watt, K.; Anderson, S.; Gianella-Borradori, A.; Lane, D. P.; Green, S. R. Seliciclib (CYC202, *R*-roscovitine) induces cell death in multiple myeloma cells by inhibition of RNA polymerase II-dependent transcription and down-regulation of Mcl-1. *Cancer Res.* **2005**, *65*, 5399–5407.

(54) Whittaker, S. R.; Te Poele, R. H.; Chan, F.; Linardopoulos, S.; Walton, M. I.; Garrett, M. D.; Workman, P. The cyclin-dependent kinase inhibitor seliciclib (*R*-roscovitine; CYC202) decreases the expression of mitotic control genes and prevents entry into mitosis. *Cell Cycle* **2007**, *6*, 3114–3131.

(55) Barrie, S. E.; Eno-Amooquaye, E.; Hardcastle, A.; Platt, G.; Richards, J.; Bedford, D.; Workman, P.; Aherne, W.; Mittnacht, S.; Garrett, M. D. High-throughput screening for the identification of small-molecule inhibitors of retinoblastoma protein phosphorylation in cells. *Anal. Biochem.* **2003**, *320*, 66–74.

(56) Raynaud, F. I.; Whittaker, S. R.; Fischer, P. M.; McClue, S.; Walton, M. I.; Barrie, S. E.; Garrett, M. D.; Rogers, P.; Clarke, S. J.; Kelland, L. R.; Valenti, M.; Brunton, L.; Eccles, S.; Lane, D. P.; Workman, P. In vitro and in vivo pharmacokinetic-pharmacodynamic relationships for the trisubstituted aminopurine cyclin-dependent kinase inhibitors olomoucine, bohemine and CYC202. *Clin. Cancer Res.* **2005**, *11*, 4875–4887.

(57) Blagosklonny, M. V. Flavopiridol, an inhibitor of transcription: implications, problems and solutions. *Cell Cycle* **2004**, *3*, 1537–1542.

(58) Sedlacek, H. H. Mechanisms of action of flavopiridol. *Crit. Rev. Oncol. Hematol.* **2001**, *38*, 139–170.

(59) Senderowicz, A. M. Flavopiridol: the first cyclin-dependent kinase inhibitor in human clinical trials. *Invest. New Drugs* **1999**, *17*, 313–320.

(60) Lane, M. E.; Yu, B.; Rice, A.; Lipson, K. E.; Liang, C.; Sun, L.; Tang, C.; McMahon, G.; Pestell, R. G.; Wadler, S. A novel cdk2-selective inhibitor, SU9516, induces apoptosis in colon carcinoma cells. *Cancer Res.* **2001**, *61*, 6170–6177.

(61) Moshinsky, D. J.; Bellamacina, C. R.; Boisvert, D. C.; Huang, P.; Hui, T.; Jancarik, J.; Kim, S. H.; Rice, A. G. SU9516: biochemical analysis of cdk inhibition and crystal structure in complex with cdk2. *Biochem. Biophys. Res. Commun.* **2003**, *310*, 1026–1031.

(62) Gojo, I.; Zhang, B.; Fenton, R. G. The cyclin-dependent kinase inhibitor flavopiridol induces apoptosis in multiple myeloma cells through transcriptional repression and down-regulation of Mcl-1. *Clin. Cancer Res.* **2002**, *8*, 3527–3538.

(63) Raje, N.; Kumar, S.; Hideshima, T.; Roccaro, A.; Ishitsuka, K.; Yasui, H.; Shiraishi, N.; Chauhan, D.; Munshi, N. C.; Green, S. R.; Anderson, K. C. Seliciclib (CYC202 or *R*-roscovitine), a small-molecule cyclin-dependent kinase inhibitor, mediates activity via down-regulation of Mcl-1 in multiple myeloma. *Blood* **2005**, *106*, 1042–1047.

(64) Gao, N.; Kramer, L.; Rahmani, M.; Dent, P.; Grant, S. The three-substituted indolinone cyclin-dependent kinase 2 inhibitor 3-[1-(3*H*-imidazol-4-yl)-meth-(*Z*)-ylidene]-5-methoxy-1,3-dihydro-indol-2-one (SU9516) kills human leukemia cells via down-regulation of Mcl-1 through a transcriptional mechanism. *Mol. Pharmacol.* **2006**, *70*, 645–655.

(65) David-Pfeuty, T.; Nouvian-Dooghe, Y.; Sirri, V.; Roussel, P.; Hernandez-Verdun, D. Common and reversible regulation of wild-type p53 function and of ribosomal biogenesis by protein kinases in human cells. *Oncogene* **2001**, *20*, 5951–5963.

(66) Kotala, V.; Uldrijan, S.; Horky, M.; Trbusek, M.; Strnad, M.; Vojtesek, B. Potent induction of wild-type p53-dependent transcription in tumour cells by a synthetic inhibitor of cyclin-dependent kinases. *Cell. Mol. Life Sci.* **2001**, *58*, 1333–1339.

(67) Helleday, T. Homologous recombination in cancer development, treatment and development of drug resistance. *Carcinogenesis* **2010**, *31*, 955–960.

(68) Huertas, P.; Cortes-Ledesma, F.; Sartori, A. A.; Aguilera, A.; Jackson, S. P. CDK targets Sae2 to control DNA-end resection and homologous recombination. *Nature* **2008**, *455*, 689–692.

(69) Ambrosini, G.; Seelman, S. L.; Qin, L. X.; Schwartz, G. K. The cyclin-dependent kinase inhibitor flavopiridol potentiates the effects of topoisomerase I poisons by suppressing Rad51 expression in a p53-dependent manner. *Cancer Res.* **2008**, *68*, 2312–2320.

(70) Deans, A. J.; Khanna, K. K.; McNees, C. J.; Mercurio, C.; Heierhorst, J.; McArthur, G. A. Cyclin-dependent kinase 2 functions in normal DNA repair and is a therapeutic target in BRCA1-deficient cancers. *Cancer Res.* **2006**, *66*, 8219–8226.

(71) Chen, F.; Nastasi, A.; Shen, Z.; Brenneman, M.; Crissman, H.; Chen, D. J. Cell cycle-dependent protein expression of mammalian homologs of yeast DNA double-strand break repair genes Rad51 and Rad52. *Mutat. Res.* **1997**, *384*, 205–211.

(72) Sartori, A. A.; Lukas, C.; Coates, J.; Mistrik, M.; Fu, S.; Bartek, J.; Baer, R.; Lukas, J.; Jackson, S. P. Human CtIP promotes DNA end resection. *Nature* **2007**, *450*, 509–514.

(73) Bartkova, J.; Horejsi, Z.; Koed, K.; Kramer, A.; Tort, F.; Zieger, K.; Guldberg, P.; Sehested, M.; Nesland, J. M.; Lukas, C.; Orntoft, T.; Lukas, J.; Bartek, J. DNA damage response as a candidate anti-cancer barrier in early human tumorigenesis. *Nature* **2005**, *434*, 864–870.

(74) Gorgoulis, V. G.; Vassiliou, L. V.; Karakaidos, P.; Zacharatos, P.; Kotsinas, A.; Liloglou, T.; Venere, M.; DiTullio, R. A., Jr.; Kastrinakis, N. G.; Levy, B.; Kletsas, D.; Yoneta, A.; Herlyn, M.; Kittas, C.; Halazonetis, T. D. Activation of the DNA damage checkpoint and genomic instability in human precancerous lesions. *Nature* **2005**, *434*, 907–913.

(75) Halazonetis, T. D.; Gorgoulis, V. G.; Bartek, J. An oncogene-induced DNA damage model for cancer development. *Science* **2008**, *319*, 1352–1355.

(76) Evans, P. Scaling and assessment of data quality. *Acta Crystallogr., Sect. D: Biol. Crystallogr.* **2006**, *62*, 72–82.

(77) McCoy, A. J.; Grosse-Kunstleve, R. W.; Adams, P. D.; Winn, M. D.; Storoni, L. C.; Read, R. J. Phaser crystallographic software. *J. Appl. Crystallogr.* **2007**, *40*, 658–674.

(78) Murshudov, G. N.; Vagin, A. A.; Dodson, E. J. Refinement of macromolecular structures by the maximum-likelihood method. *Acta Crystallogr., Sect. D: Biol. Crystallogr.* **1997**, *53*, 240–255.

(79) Adams, P. D.; Afonine, P. V.; Bunkoczi, G.; Chen, V. B.; Davis, I. W.; Echols, N.; Headd, J. J.; Hung, L. W.; Kapral, G. J.; Grosse-Kunstleve, R. W.; McCoy, A. J.; Moriarty, N. W.; Oeffner, R.; Read, R. J.; Richardson, D. C.; Richardson, J. S.; Terwilliger, T. C.; Zwart, P. H. PHENIX: a comprehensive Python-based system for macromolecular structure solution. *Acta Crystallogr., Sect. D: Biol. Crystallogr.* **2010**, *66*, 213–221.

(80) Emsley, P.; Cowtan, K. Coot: model-building tools for molecular graphics. *Acta Crystallogr., Sect. D: Biol. Crystallogr.* **2004**, *60*, 2126–2132.
(81) Pierce, A. J.; Johnson, R. D.; Thompson, L. H.; Jasin, M. XRCC3 promotes homology-directed repair of DNA damage in mammalian cells. *Genes Dev.* **1999**, *13*, 2633–2638.